Nonabelian magnonics in antiferromagnets

Matthew W. Daniels,[1,*] Ran Cheng,[1,2] Weichao Yu (余伟超),[3] Jiang Xiao (萧江),[3,4,5] and Di Xiao[1]

[1]*Department of Physics, Carnegie Mellon University, Pittsburgh, Pennsylvania 15213, USA*

[2]*Department of Electrical and Computer Engineering, Carnegie Mellon University, Pittsburgh, Pennsylvania 15213, USA*

[3]*Department of Physics and State Key Laboratory of Surface Physics, Fudan University, Shanghai 200433, China*

[4]*Collaborative Innovation Center of Advanced Microstructures, Nanjing 210093, China*

[5]*Institute for Nanoelectronics Devices and Quantum Computing, Fudan University, Shanghai 200433, China*

(Received 24 January 2018; revised manuscript received 13 August 2018; published 31 October 2018)

We present a semiclassical formalism for antiferromagnetic (AFM) magnonics which promotes the central ingredient of *spin wave chirality*, encoded in a quantity called magnonic isospin, to a first-class citizen of the theory. We use this formalism to unify results of interest from the field under a single chirality-centric formulation. Our main result is that the isospin is governed by unitary time evolution, through a Hamiltonian projected down from the full spin wave dynamics. Because isospin is SU(2) valued, its dynamics on the Bloch sphere are precisely rotations, which, in general, do not commute. Consequently, the induced group of operations on AFM spin waves is nonabelian. This is a paradigmatic departure from ferromagnetic magnonics, which operates purely within the abelian group generated by spin wave phase and amplitude. Our investigation of this nonabelian magnonics in AFM insulators focuses on studying several simple gate operations, and offering in broad strokes a program of study for interesting new logic families in antiferromagnetic spin wave systems.

DOI: 10.1103/PhysRevB.98.134450

I. INTRODUCTION

Recent years have seen a surge of interest in the generation and in-flight manipulation of magnons in antiferromagnets (AFMs). We now know that AFM magnons can couple to the angular momentum carried by electrons [1,2], photons [3–5], and other spin carriers. Detection of magnon-mediated spin signals from AFM insulators, typically measured through the inverse spin Hall effect, has also matured to the point of experimental implementation [6–8]. It has been shown that AFM spin waves possess pointed dynamical distinctions from their ferromagnetic (FM) counterpart [9–11], especially in the presence of spin texture [12–17] or broken inversion symmetry [11,12,18,19]. In particular, collinear AFMs possess two degenerate spin wave eigenmodes of opposite chirality [20]. They are often referred to as right- and left-handed modes, according to the precessional handedness of the Néel vector (Fig. 1). This notion of *spin wave chirality* has proved to be a useful narrative tool for understanding how AFM magnonics differs from the ferromagnetic (FM) case.

As a patchwork of novel results begins to populate the field of AFM magnonics, a coherent framework for understanding their similarities, differences, and possible extensions becomes necessary. Our central thesis is that many of these results can be understood in terms of spin wave chirality, through a spinor [SU(2)-valued] quantity we refer to as the *magnon isospin*. One important corollary of this formulation is that, because isospin dynamics proceeds by intrinsically noncommutative unitary rotations on the Bloch sphere, implementations of magnonic computing in AFMs will in general be nonabelian. This fundamental departure from the behavior of FM magnonics calls for a serious reinvestigation of primitive magnonic operations for AFMs; working only off analogies to extant ferromagnetic proposals is a program restricted by commutativity, and inevitably lifts only into a small subset of available AFM computing schemes.

One practical disadvantage of FM magnonics has been the need to constantly refresh the signal power in a device. This is particularly problematic in interferometric [21,22] spin wave logic, where the Boolean output of FM magnonic logic gates is encoded by setting a threshold amplitude for the spin wave power. Phase interference techniques are then used to achieve the desired magnon amplitude. Since half of the desired outputs are represented by suppressing the power spectrum of the magnon signal, this scheme incurs significant energy inefficiencies and requires sources of power to constantly refresh the signal [23]. Isospin computing resolves this problem neatly since we can encode and manipulate data in the spin wave chirality rather than the spin wave amplitude. This improvement is reminiscent of proposals for polarization-based optical computing schemes from the 1980's [24]. A chief practical distinction between AFM isospin computing and optical computing is that the former can be carried out in nanoscale solid-state systems.

Given the importance of the isospin in AFM magnonics, we consider in this paper its dynamics for a broad class of interactions that may manifest in AFMs, and offer an extensible formalism by which others can easily incorporate the effects of new physical interactions. In the development of this formalism, we find that there are notable differences between bipartite and synthetic AFMs, and we discuss the advantages

*Corresponding author: danielsmw@protonmail.com

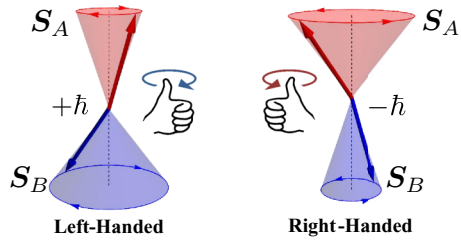

FIG. 1. Schematic representations of right- and left-handed modes. Red and blue arrows demonstrate the spin precession on each of the two sublattices. Because the $\hat{S}_z$ components differ between the sublattices during a spin wave precession, each eigenmode carries an opposite sign of spin angular momentum.

and disadvantages of pursuing nonabelian magnonics in these two types of systems. We then apply this formalism to a number of examples, for the threefold purposes of illustrating its use, validating it against a set of known results, and generating results in a few interesting systems.

With several concrete results in hand, we then propose in broad strokes a program of next-generation computing based on nonabelian magnonics [25]. Although FM magnonics has been studied extensively [21,22,26,27], we show that the comparative richness of the AFM isospin offers dramatically more and different avenues for progress. The fact that isospin manipulations do not commute offers, by purely algebraic considerations, a more bountiful landscape for composition of logical operations than can be found in FMs.

We emphasize that the dual-sublattice nature of AFMs does not *merely* amount to two copies of FM magnon systems. Although one may be able to import FM magnonic schemes into the AFM architecture, one could also look to more spinful classes of physics for inspiration in application. Spintronic [11] and optical [12] analogies to AFM magnonics have proved inspiring for novel device designs. We close by offering possibilities for future research in this direction.

II. FORMALISM

In this section, we review the AFM spin wave theory in the sublattice formalism, as we expect many of our readers are more familiar with the staggered-order-centric approach. We begin by exploring spin wave chirality in a minimal model: a collinear AFM with easy axis anisotropy. The description of easy-axis AFMs such as MnF_2, FeF_2, or Cr_2O_3 may follow from such a model. Using this familiar context, we review chirality and the way in which it encodes spin carried by the magnon excitation. We then review a common formalism for handling spin texture and introduce the texture-induced gauge fields. Finally, we derive the spin wave equations of motion in the sublattice formalism by the variational principle. These subsections set the stage for our main results, which are presented in the next section.

A. Sublattice-centric magnonics

In terms of the two sublattices, the free energy of an easy-axis collinear AFM in the continuum limit is

$$F = F_{\text{exch}} + F_{\text{EAA}}, \tag{1a}$$

$$F_{\text{exch}} = \frac{1}{2}\int Z\mathbf{m}_A\cdot\mathbf{m}_B - J\nabla\mathbf{m}_A\cdot\nabla\mathbf{m}_B\, d^d\mathbf{x}, \tag{1b}$$

$$F_{\text{EAA}} = -\frac{K}{2}\int (\mathbf{m}_A\cdot\hat{z})^2 + (\mathbf{m}_B\cdot\hat{z})^2\, d^d\mathbf{x}. \tag{1c}$$

Here, K is the easy-axis anisotropy (EAA), while Z and J are the so-called homogeneous and inhomogeneous exchange interactions, respectively [28]. They have been chosen so that, under the change of variables

$$\mathbf{m} = \frac{\mathbf{m}_A + \mathbf{m}_B}{2} \quad \text{and} \quad \mathbf{n} = \frac{\mathbf{m}_A - \mathbf{m}_B}{2}, \tag{2}$$

the exchange free-energy density becomes [29]

$$\mathcal{F}_{\text{exch}} = Z|\mathbf{m}|^2 + \frac{J}{2}|\nabla\mathbf{n}|^2 + O(|\mathbf{m}|^4). \tag{3}$$

The quantities $\mathbf{m}$ and $\mathbf{n}$ are the local magnetization and the staggered order [30]. We have written in Eq. (1) a free energy for the classic g-type antiferromagnet, but merely as a convenient concretization. Our main result generalizes to any kind of collinear AFM order, and in particular we use results for synthetic AFMs later in the paper.

On each sublattice of the AFM, the semiclassical spin dynamics is governed by the Landau-Lifshitz equation

$$\dot{\mathbf{m}}_A = \mathbf{m}_A \times \frac{1}{S}\frac{\delta F}{\delta \mathbf{m}_A}, \tag{4a}$$

$$\dot{\mathbf{m}}_B = \mathbf{m}_B \times \frac{1}{S}\frac{\delta F}{\delta \mathbf{m}_B}, \tag{4b}$$

where F is the free-energy functional and $S = s\hbar$ the spin magnitude on a lattice site. Define $\hat{z}$ as the easy-axis direction, and take the Néel ground state as $\mathbf{m}_A = \hat{z}$ and $\mathbf{m}_B = -\hat{z}$. Spin wave fluctuations, at linear order in the cone angle by which precessing spins cant away from the ground state, reside entirely in the xy plane [31]. It is convenient to rewrite fluctuations from equilibrium as $\alpha_\pm = (m_A^x \pm i m_A^y)/\sqrt{2}$ and $\beta_\pm = (m_B^x \pm i m_B^y)/\sqrt{2}$. We will treat these four quantities as independent variables [32]. Collecting the equations of motion for this new basis [33] into matrix form, the spin wave equations for $\Psi = (\alpha_+, \beta_+, \alpha_-, \beta_-)$ are

$$i(\tau_z \otimes \sigma_z)\dot{\Psi} = \begin{pmatrix} \hat{h} & 0 \\ 0 & \hat{h}^* \end{pmatrix}\Psi = \mathcal{H}\Psi, \tag{5}$$

where τ_j are the Pauli matrices in isospin space and σ_j the Pauli matrices in the sublattice subspace. In other words, the σ_j matrices distinguish α_+ from β_+ and α_- from β_-, while τ_j distinguish from α_+ from α_- and β_+ from β_-. Our use of the term "isospin" will be introduced more fully at the end of this section. For the problem we outlined above, $\hat{h}$ is a 2×2 Hermitian operator given by

$$\hat{h} = \tfrac{1}{2}[(Z+2K)\mathbb{1}_2 + \sigma_x(Z + J\nabla^2)]. \tag{6}$$

For the simple free energy we have adopted in Eq. (1), Eq. (5) apparently contains two copies of the same two-level dynamics. These two copies are related by complex conjugation, which we write as the time-reversal operator $\mathcal{T}$.

The mapping of the Landau-Lifshitz-Gilbert (LLG) equation onto a Schrödinger equation is standard practice in theoretical magnonics [34,35], but note that our Eq. (5) differs from the usual Schrödinger equation by the appearance of $\tau_z \otimes \sigma_z$ on the left-hand side. The mathematical and philosophical details of Schrödinger equations with this structure have been considered at length in Ref. [36].

Since the Hamiltonian (5) is block diagonal, let us first focus on the subspace governing α_+ and β_+. Assuming our system is stationary and translationally invariant, we can make the ansatz $\psi = \psi_0 e^{i(\mathbf{k}\cdot\mathbf{x}-\omega t)}$. The resulting eigenproblem is

$$\hbar\omega\sigma_z\psi = \hat{h}\psi. \tag{7}$$

For a generic 2×2 Hermitian operator $\hat{h} = a\mathbb{1}_2 + b\sigma_x + c\sigma_y + d\sigma_z$, Eq. (7) has the solution [18]

$$\psi_0 = \begin{pmatrix} \cosh\frac{\vartheta}{2} \\ -e^{i\varphi}\sinh\frac{\vartheta}{2} \end{pmatrix} \quad \text{and} \quad \psi_1 = \begin{pmatrix} -\sinh\frac{\vartheta}{2} \\ e^{i\varphi}\cosh\frac{\vartheta}{2} \end{pmatrix}, \tag{8}$$

where the angles ϑ and φ are given through

$$a = \ell\cosh\vartheta, \tag{9a}$$

$$b = \ell\sinh\vartheta\cos\varphi, \tag{9b}$$

$$\text{and } c = \ell\sinh\vartheta\sin\varphi. \tag{9c}$$

The corresponding eigenvalues are

$$\hbar\omega = \pm(d+\ell) = \pm\frac{1}{S}\sqrt{\frac{1}{2}JZk^2 + ZK} \tag{10}$$

at leading order in K. The well-known resonant energy is given then by $\hbar\omega_0 = \sqrt{ZK}/S$.

We note that the bosonic normalization condition [18,37,38] $a^2 - b^2 - c^2 = \pm 1$ implies that the space of Hamiltonians, as well as the eigenvectors themselves, live on the hyperboloid of two sheets SU(1,1). When $d = 0$, as in Eq. (6), the eigenvectors have particle-hole symmetry. ψ_j exhibits eigenfrequency $(-)^j|\omega|$. Analysis of the basis functions shows that ψ_0 is a right-handed precession of $\mathbf{m}_A$ (and therefore $\mathbf{n}$) while ψ_1 is a left-handed precession. We say that they have opposite chirality, namely, right-handed and left-handed chirality.

Notice that the sister eigenproblem (for α_- and β_-) in the lower two rows of Eq. (5) has positive frequency solutions corresponding to left-handed modes and negative frequency solutions corresponding to right-handed modes. This inversion from the $\{\alpha_+, \beta_+\}$ problem arises precisely due to the conjugate basis. We will take the positive-energy solution from each block,

$$\Psi_0 = \begin{pmatrix} \cosh\frac{\vartheta}{2} \\ -e^{i\varphi}\sinh\frac{\vartheta}{2} \\ 0 \\ 0 \end{pmatrix} \quad \text{and} \quad \Psi_1 = \begin{pmatrix} 0 \\ 0 \\ -\sinh\frac{\vartheta}{2} \\ e^{i\varphi}\cosh\frac{\vartheta}{2} \end{pmatrix}, \tag{11}$$

as a chirally complete basis for the positive energy, degenerate Hilbert subspace of Eq. (5). Note that whereas the solutions (8) obey $\langle\psi_i|\sigma_z|\psi_j\rangle = (-)^j\delta_{ij}$, the solutions $\langle\Psi_i|\tau_z\otimes\sigma_z|\Psi_j\rangle = \delta_{ij}$ are properly normalizable. We will often work directly in the Ψ_0 and Ψ_1 basis, writing $|0\rangle = (1,0)$ and $|1\rangle = (0,1)$ as in Fig. 2. The use of bra-ket notation here

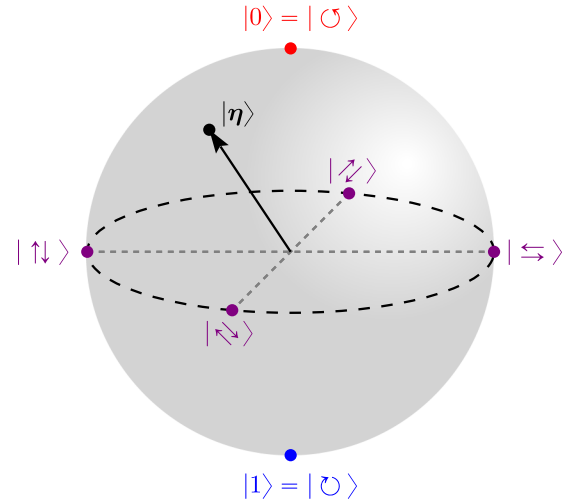

FIG. 2. Linear combinations of the right- and left-handed modes $|0\rangle \cong \Psi_0$ and $|1\rangle \cong \Psi_1$, respectively, produce an entire Bloch sphere's worth of possible isospin states. We have labeled selected states by the polarization of the Néel order fluctuations in that state. Right- and left-handed modes correspond to right- and left-handed precession of $\mathbf{n}$, while equal linear combinations produce linearly polarized waves. The angle of linear polarization depends on the relative phase of the spin waves between the sites. Note that X- and Y-polarized states are orthogonal here, while in a traditional quantum spin space $|X\rangle$ is orthogonal to $|-X\rangle$, not $|Y\rangle$. Since our formalism parametrizes this space in terms of a two-level spinor, we refer to it as a Bloch sphere. Students of optics, however, will recognize that it is analogous to the Poincaré sphere that parametrizes optical polarization states.

is a formalism of convenience arising from the close mathematical similarities between our system and single-particle quantum mechanics. However, we emphasize early on that this is a purely notational convenience; it is impossible to realize many-body quantum phenomena, such as entanglement, in a purely semiclassical magnonic system.

Since $\cosh x > \sinh x$ for all real x, the magnitude of the spin wave precession is clearly dominated by the A sublattice in Ψ_0 and the B sublattice in Ψ_1. The physical spin fluctuations can be recovered by taking $m_A^x = \mathrm{Re}[(\alpha_+ + \alpha_-)/\sqrt{2}]$, $m_A^y = \mathrm{Re}[(\alpha_+ - \alpha_-)/\sqrt{2}i]$, and likewise with the B sublattice, so that

$$\boldsymbol{\delta m}_A^{(0)} = \frac{1}{\sqrt{2}}(\cos(\omega t), \sin(\omega t))\cosh\frac{\vartheta}{2}, \tag{12a}$$

$$\boldsymbol{\delta m}_B^{(0)} = -\frac{1}{\sqrt{2}}(\cos(\omega t - \varphi), \sin(\omega t - \varphi))\sinh\frac{\vartheta}{2}, \tag{12b}$$

$$\boldsymbol{\delta m}_A^{(1)} = -\frac{1}{\sqrt{2}}(\cos(\omega t), -\sin(\omega t))\sinh\frac{\vartheta}{2}, \tag{12c}$$

$$\boldsymbol{\delta m}_B^{(1)} = \frac{1}{\sqrt{2}}(\cos(\omega t - \varphi), -\sin(\omega t - \varphi))\cosh\frac{\vartheta}{2}. \tag{12d}$$

We see in Eqs. (12) that the right-handed modes dominate on the A sublattice, as in Fig. 1. One can also see from Fig. 1 that these two modes carry opposite magnetization since the $\hat{S}_z$ component of the sublattices must differ if one of the sublattices dominates. The reduction of magnetization on each

sublattice is simply given by the squared magnitude of the lattice spin wave, so that the total magnetization induced by a spin wave is

$$m_z = -S\langle\Psi|(\mathbb{1}_2 \otimes \sigma_z)|\Psi\rangle, \tag{13}$$

which will be negative for right-handed waves proportional to Ψ_0 and positive for left-handed waves proportional to Ψ_1. This operator $\mathbb{1}_2 \otimes \sigma_z$ corresponds to a so-called nongeometric symmetry [39]. It has sometimes been given as the *definition* of spin wave chirality. In electromagnetic analogies for AFM spin wave dynamics it corresponds to optical helicity [39], where the corresponding conserved quantity is the so-called zilch [40].

So far, we have dealt only with a block-diagonal Hamiltonian. Restricting to the positive energy subspace, we see that $\mathcal{H}$ has no off-diagonal terms that connect Ψ_0 and Ψ_1. If such terms existed, we could manipulate the total spin carried by the spin wave in transit, rotating our spin wave state within the degenerate eigensubspace. We may imagine that the coefficients balancing these eigenvectors in a superposition $|\boldsymbol{\eta}\rangle = \eta_0|0\rangle + \eta_1|1\rangle$ define a degree of freedom which we refer to as the magnonic isospin [41]. *The desire to exploit this internal degree of freedom motivates the remainder of the paper.*

B. Spin texture, characteristic length scales, and perturbative parameters

In order to control $\boldsymbol{\eta}$, we must find a way to break the degeneracy between the right- and left-handed modes; that is, we must break whatever symmetries are protecting either conservation of chirality (that is, the block diagonality of $\mathcal{H}$) or conservation of the relative phase between right- and left-handed modes. In this paper, the main tools we consider for this purpose are spin texture and the Dzyaloshinskii-Moriya interaction (DMI). The latter is well known and we introduce the appropriate free energies when they are needed. Spin texture, however, is somewhat more subtle, so we briefly review theoretical tools for handling it. These techniques have been used to great success in describing transport effects arising from both ferromagnetic [34,35,42,43] and antiferromagnetic [44–46] textures.

To describe the spin texture in our formalism, we encode the texture in a rotation matrix R defined by $R\mathbf{n} = |\mathbf{n}|\hat{z}$. This rotation matrix induces a generator of infinitesimal spin rotations $(\partial_\mu R)R^T$, which itself can be regarded as a collection of vector potentials $A^x_\mu J_x + A^y_\mu J_y + A^z_\mu J_z = (\partial_\mu R)R^T$, the decomposition being directed through the standard generators [47] of three-dimensional (3D) rotations J_j. Here, μ is a spacetime index, and the components A^j_μ define the $(1+d)$-vectors $A^j = (A^j_t, \mathbf{A}^j)$.

Because our spin texture is described with respect to the $\hat{z}$ axis, $\mathbf{A}^z$ will be of paramount importance. It gives rise to an emergent magnetic field $\mathbf{B} = \boldsymbol{\nabla} \times \mathbf{A}^z$ that produces a Lorentz force on magnons in Eqs. (27), and the temporal component A^z_t likewise produces an emergent electric field. We will usually describe the influence of the other two potentials through the complex variable $\mathcal{A}_\mu = (A^x_\mu + iA^y_\mu)/\sqrt{2}$. For more information on these fields, the reader is referred to Appendix B. For a full discussion of this gauge field formalism in the treatment of spin texture, the reader may check Refs. [34,35].

We will soon need an approximation scheme to deal with the many perturbative effects (anisotropy, DMI, etc.) of our spin wave system. Since A^j_μ is a derivative of the texture-defining angles, let it define a characteristic length scale λ of the system,

$$|A^j_\mu| \sim \frac{1}{\lambda}. \tag{14}$$

In textured systems with DMI, the characteristic length scale is proportional [48] to J/D, where D is the DMI strength [49] $\mathcal{F}_{\rm DMI} = D\mathbf{m}_A \cdot (\boldsymbol{\nabla} \times \mathbf{m}_B)$. Therefore [50],

$$D/J \sim |A^j_\mu|. \tag{15}$$

In systems with easy-axis anisotropy, meanwhile, the well-known characteristic length of a domain wall is $\sqrt{J/K}$, and thus

$$K/J \sim |A^j_\mu|^2. \tag{16}$$

Finally, the local magnetization [51] $\mu = (R\mathbf{m}) \cdot (\hat{x} + i\hat{y})/\sqrt{2}$ scales as a derivative of the staggered order, [28]

$$\mu \sim |A^j_\mu|. \tag{17}$$

As it happens, the magnetization will, in our calculations, never show up as a lone linear-order term; even so, the quadratic terms $O(\mu^2) = O(K/J)$ must be preserved.

We have established a hierarchy of perturbative orders based on a single parameter $|A|$. In our spin wave treatment, we will keep terms up to order $\partial A \sim O(A^2)$, that is, to linear order in the emergent electromagnetic field $\mathbf{B} = \boldsymbol{\nabla} \times \mathbf{A}^z$.

C. Matrix structure of the spin wave Hamiltonian

Once we add extra terms to the free energy (spin texture, the Dzyaloshinskii-Moriya interaction, and so on) the equation of motion becomes

$$i(\tau_z \otimes \sigma_z)\dot{\Psi} = \frac{\epsilon^d}{nS}\frac{\delta F}{\delta \bar{\Psi}} - A^z_t(\mathbb{1}_2 \otimes \sigma_z)\Psi \tag{18}$$

so that the spin wave Hamiltonian is given through $\mathcal{H}\Psi = \delta F/\delta\bar{\Psi}$. Here, ϵ is the lattice constant, d is the dimensionality of the lattice, and $n = 1 + |\mu|^2$ is the effective index of refraction for the spin wave speed, when viewed from the perspective of the wave equation governing staggered order dynamics. Equation (18) prescribes the correct harmonic spin wave theory for any free energy F, where the independent variables $\{\alpha_+, \beta_+, \alpha_-, \beta_-\}$ are now defined as the *purely in-plane* fluctuations of the sublattice spin wave modes after the active rotation by R of the ground-state texture. The detailed derivation of Eq. (18) is given in Appendix A.

For concreteness, we now present the detailed matrix form of the exchange interaction Hamiltonian. Beginning from Eq. (1b), we rotate the fields by R and change variables to the in-plane complex fluctuations α_+, β_+, α_-, and β_-. The corresponding Hamiltonian for the homogeneous exchange

interaction is

$$\mathcal{H}_{\text{hom}} = \frac{Z}{2}\begin{pmatrix} 1-3|\mu|^2 & 1-|\mu|^2 & \mu^2 & -\mu^2 \\ 1-|\mu|^2 & 1-3|\mu|^2 & -\mu^2 & \mu^2 \\ \bar{\mu}^2 & -\bar{\mu}^2 & 1-3|\mu|^2 & 1-|\mu|^2 \\ -\bar{\mu}^2 & \bar{\mu}^2 & 1-|\mu|^2 & 1-3|\mu|^2 \end{pmatrix}, \tag{19}$$

where the bar over $\bar{\mu}$ (and, later, over $\bar{\mathcal{A}}$) indicates complex conjugation. The inhomogeneous exchange interaction $\mathcal{H}_{\text{inhom}}$, meanwhile, is given by $J/(2n)$ times the matrix

$$\begin{pmatrix} -2|\mathcal{A}|^2 & (\nabla - i\mathbf{A}^z)^2 + \boldsymbol{\Delta}\cdot\nabla - |\mathcal{A}|^2 & 0 & -(\mu\nabla)^2 + 4i\mu\mathcal{A}\cdot\nabla + \mathcal{A}^2 \\ (\nabla - i\mathbf{A}^z)^2 - \boldsymbol{\Delta}\cdot\nabla - |\mathcal{A}|^2 & -2|\mathcal{A}|^2 & -(\mu\nabla)^2 - 4i\mu\mathcal{A}\cdot\nabla + \mathcal{A}^2 & 0 \\ 0 & -(\bar{\mu}\nabla)^2 + 4i\bar{\mu}\bar{\mathcal{A}}\cdot\nabla + \bar{\mathcal{A}}^2 & -2|\mathcal{A}|^2 & (\nabla + i\mathbf{A}^z)^2 + \boldsymbol{\Delta}\cdot\nabla - |\mathcal{A}|^2 \\ -(\bar{\mu}\nabla)^2 - 4i\bar{\mu}\bar{\mathcal{A}}\cdot\nabla + \bar{\mathcal{A}}^2 & 0 & (\nabla + i\mathbf{A}^z)^2 - \boldsymbol{\Delta}\cdot\nabla - |\mathcal{A}|^2 & -2|\mathcal{A}|^2 \end{pmatrix}, \tag{20}$$

where $\boldsymbol{\Delta} = 2i(\bar{\mu}\mathcal{A} - \mu\bar{\mathcal{A}})$. These matrix Hamiltonians, and the Hamiltonians corresponding to any other two-site interaction, exhibit notable structural differences when the synthetic AFM case is considered instead. In the Supplemental Material, we have provided a *Mathematica* notebook that automates the derivation of $\mathcal{H}$ for any free energy given in terms of $\mathbf{m}_A$ and $\mathbf{m}_B$ [52]. It also contains precomputed Hamiltonians for anisotropy, DMI, external fields, and so on, which we use in our applied examples later in the paper.

III. NONABELIAN WAVE-PACKET THEORY

In this section, motivated by the need to derive $\boldsymbol{\eta}$ dynamics from Eq. (18) in the case of spatial inhomogeneity, we apply the machinery of nonabelian wave-packet theory [53]. What we call "wave-packet theory" was originally developed in a paper by Chang and Niu [54] to explain the Hofstadter butterfly spectrum, after which their treatment was codified by Ref. [55]. Since then, the theory has been applied in a variety of contexts, sometimes requiring extensions of the theory to account for unique features of a particular physical problem [56–58].

The most relevant extension for our purposes, and indeed, one of the most ambitious and interesting developments in wave-packet theory, is the treatment of multiple degenerate bands [53,59]. In this case, the theory is called *nonabelian wave-packet theory* because, in dealing with a vector of multiple band energies at once, the "coefficients" must become matrix valued (and therefore, generally speaking, an element of a nonabelian matrix representation) in order to act on the multiband wave function. In this paper, we extend the nonabelian wave-packet theory to account for both the unusual $\tau_z \otimes \sigma_z$ factor in our Lagrangian and our explicitly *a priori* nonabelian gauge field [60]. A detailed derivation involving the internal workings of wave-packet theory is crucial for establishing our main results. Since details of wave-packet theory, even in the abelian case, are not widely studied, we carefully guide the interested reader through the derivation in Appendix D.

The basic idea of abelian wave-packet theory is to consider a momentum-space superposition $|W\rangle = \int w_q \psi_q \, d^d\mathbf{q}$ of eigenvectors, where the eigenvectors are drawn from the spectrum of the Hamiltonian evaluated at some $(\mathbf{x}_c, \mathbf{q}_c)$ on a classical phase space. In nonabelian wave-packet theory, the eigenvector is expressed as a general state lying in the degenerate subspace spanned by our right- and left-handed modes

$$|W(\mathbf{x}_c, \mathbf{k}_c)\rangle = \int d\mathbf{q}\, w(\mathbf{q}, t)[\eta_0(\mathbf{q}, t)|\Psi_0(\mathbf{q}, t)\rangle + \eta_1(\mathbf{q}, t)|\Psi_1(\mathbf{q}, t)\rangle]. \tag{21}$$

The coefficient w gives the shape of the wave packet, as in Fig. 3. The vector $|\boldsymbol{\eta}\rangle = (\eta_0, \eta_1)$ is, again, called the *isospin*. We demand that the otherwise generic wave packet possess

(1) a momentum space distribution localized enough to be approximated as $\delta(\mathbf{q} - \mathbf{q}_c)$,

(2) a well-defined mean position $\mathbf{x}_c = \langle W|\hat{\mathbf{x}}|W\rangle$, and

(3) sufficient spatial localization that the environment where the wave packet has appreciable support is approximately translationally invariant.

These assumptions form a set of sufficient conditions under which a wave function's semiclassical dynamics can be formulated, using wave-packet theory, on a classical phase space $\Gamma \ni (\mathbf{x}_c, \mathbf{q}_c)$. The nonabelian version, Eq. (D13), includes an $\boldsymbol{\eta}$-valued fiber over Γ.

By appealing to the time-dependent variational principle, we can write the Lagrangian which generates the equation of motion (18), namely, $L_{\text{WP}} = \langle\Psi|\mathcal{L}|\Psi\rangle$ with

$$\mathcal{L} = i(\tau_z \otimes \sigma_z)\frac{d}{dt} - \mathcal{H} - A_t^z\sigma_z. \tag{22}$$

We then assume $|W\rangle$ as the solution for $|\Psi\rangle$. Since the wave packet is sufficiently [61] described by the 3-tuple $(\mathbf{x}_c, \mathbf{q}_c, \boldsymbol{\eta})$, we can reduce L_{WP} to a Lagrangian of the phase-space variables $\mathbf{x}_c$, $\mathbf{q}_c$, and $\boldsymbol{\eta}$ that specify $|W\rangle$. The result is

$$L_{\text{WP}} = L_{dt} + L_H + L_{\text{EM}}, \text{ where} \tag{23a}$$

$$L_{dt} = \langle\tilde{\boldsymbol{\eta}}|\dot{\mathbf{x}}_c\cdot\hat{a}_{\mathbf{x}} + \dot{\mathbf{q}}_c\cdot\hat{a}_{\mathbf{q}} + \hat{a}_t + i\partial_t|\tilde{\boldsymbol{\eta}}\rangle - \dot{\mathbf{q}}_c\cdot\mathbf{x}_c, \tag{23b}$$

$$L_H = -\langle\boldsymbol{\eta}|\mathscr{H}|\boldsymbol{\eta}\rangle, \tag{23c}$$

$$L_{\text{EM}} = -\dot{\mathbf{A}}^z\cdot\Gamma_{\mathbf{q}} - \chi\left(\dot{\mathbf{A}}^z\cdot\mathbf{x}_c + A_t^z\right). \tag{23d}$$

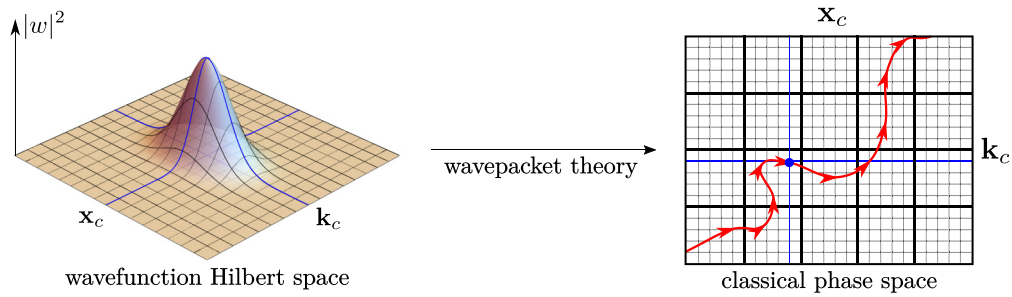

FIG. 3. Under the assumptions of wave-packet theory, the magnon wave packet has its magnitude $w(\mathbf{q}, t)$ strongly localized in real and momentum space. Consequently, the wave function is sufficiently specified by its mean coordinates $(\mathbf{x}_c, \mathbf{k}_c)$ on phase space. The wave-packet theory machinery uses this assumption to resolve the wave theory (left) described by Eq. (18) into a particle theory (right) described by the classical Lagrangian (23). Not pictured is the isospin degree of freedom, which lives in an SU(2) fiber over the classical phase space. The full semiclassical dynamics described by Eqs. (27) occurs on the induced fiber bundle.

L_{dt}, L_H, and L_{EM} derive from the time derivative, Hamiltonian, and emergent field terms from Eq. (22), respectively. Here in the main text, we simply pause to describe the various physical variables in Eqs. (23) that fall out of the derivation.

First, let us define the 4×2 matrix

$$E = |0\rangle\langle\Psi_0| + |1\rangle\langle\Psi_1|, \tag{24}$$

where $|0\rangle$ and $|1\rangle$ are understood as the basis vectors (1,0) and (0,1) for the isospin $|\boldsymbol{\eta}\rangle = \eta_0|0\rangle + \eta_1|1\rangle$. E is essentially a change of basis matrix (which chooses Ψ_0 and Ψ_1 as the canonical basis vectors), followed by a projection to the forward-time degenerate Hilbert subspace that they span. $E^\dagger$ represents the embedding of the isospin dynamics into the full spin wave dynamics, and as such the induced isospin Hamiltonian is given by

$$\mathscr{H} = E\mathcal{H}E^\dagger. \tag{25}$$

Next, we define the various 2×2 matrices $\hat{a}_\mu$. These are the matrix-valued Berry connections in isospin space

$$\hat{a}^{ij}_\mu = \left\langle \Psi^i_{\mathbf{q}} \middle| i\sigma_z \partial_\mu \Psi^j_q \right\rangle. \tag{26}$$

These diagonal matrices will generate Berry curvatures (effective, emergent magnetic fields) in the equations of motion [53]. The term $\Gamma_{\mathbf{q}} = \langle\boldsymbol{\eta}|\tau_z\hat{a}_{\mathbf{q}}|\boldsymbol{\eta}\rangle - \langle\boldsymbol{\eta}|\tau_z|\boldsymbol{\eta}\rangle\langle\boldsymbol{\eta}|\hat{a}_{\mathbf{q}}|\boldsymbol{\eta}\rangle$ arises uniquely due to the $\tau_z \otimes \sigma_z$ metric structure of our full four-dimensional Hilbert space, and is absent from existing nonabelian wave-packet theories which deal only with Euclidean spaces. It gives rise to a nonlinear potential $V_\chi = \delta\Gamma_{\mathbf{q}}/\delta\boldsymbol{\eta}$. Finally, the tilde decoration on $\tilde{\boldsymbol{\eta}} = \mathcal{G}\boldsymbol{\eta}$ refers to a gauge transformation $\mathcal{G} = \exp[-i(\tau_z \otimes \mathbb{1}_2)\mathbf{A}^z \cdot \mathbf{x}]$ discussed in Eq. (D9). Hamilton's principle $\delta S = 0$ gives us equations of motion for the dynamical variables:

$$\dot{\mathbf{q}}_c = \chi(\mathbf{E} + \dot{\mathbf{x}}_c \times \mathbf{B}) - \frac{\partial \mathcal{E}}{\partial \mathbf{x}_c}, \tag{27a}$$

$$\dot{\mathbf{x}}_c = \frac{\partial \mathcal{E}}{\partial \mathbf{q}_c} + \langle\boldsymbol{\Omega}^{\mathbf{qq}}\rangle\dot{\mathbf{q}}_c + \langle\boldsymbol{\Omega}^{\mathbf{qx}}\rangle\dot{\mathbf{x}}_c + \langle\Omega^{\mathbf{q}t}\rangle, \tag{27b}$$

$$i\frac{d}{dt}\boldsymbol{\eta} = \left[\mathscr{H} - \mathscr{A}_t + \tau_z A^z_t + \hat{V}_\chi\right]\boldsymbol{\eta}, \tag{27c}$$

with $\mathscr{A}_t = \dot{\mathbf{x}}_c \cdot \hat{a}_{\mathbf{x}} + \dot{\mathbf{q}}_c \cdot \hat{a}_{\mathbf{q}} + \hat{a}_t$, $\mathcal{E}$ the linearly perturbed spin wave energy (as in Ref. [53]), and $\boldsymbol{\Omega}$ are the various Berry curvature terms

$$\left\langle \Omega^{\alpha\beta}_{\mu\nu} \right\rangle = \langle\boldsymbol{\eta}| \left(\frac{\partial \hat{a}_{\beta^\nu}}{\partial \alpha^\mu} - \frac{\partial \hat{a}_{\alpha^\mu}}{\partial \beta^\nu} \right) |\boldsymbol{\eta}\rangle. \tag{28}$$

Finally, the emergent electromagnetic fields are $\mathbf{B} = \boldsymbol{\nabla} \times \mathbf{A}^z$ and $\mathbf{E} = \boldsymbol{\nabla} A^z_t$, familiar to those who have studied magnetic skyrmion physics [35,62].

The reduction of L_{WP} to single-particle Lagrangian (23) is quite technical, and we relegate the derivation to Appendix D. The process is illustrated schematically in Fig. 3. The equations of motion (27), as well as their derivation, are tightly related to the results of Ref. [53]. The differences arise due to the non-Euclidean metric $\tau_z \otimes \sigma_z$ in the Lagrangian. This geometry gives rise to the dynamical charge $\chi = \langle\boldsymbol{\eta}|\tau_z|\boldsymbol{\eta}\rangle$ coupled to the Lorentz force, and also gives rise to the nonlinear potential V_χ (through $\Gamma_{\mathbf{q}}$).

Although V_χ can contribute at $O(\mathbb{A}^2)$ in perturbation theory in principle, it only contributes at third order or above for the interactions we consider concretely in this paper. To contribute in our formalism, it would require that $\hat{a}_{\mathbf{q}}$ manifest at leading order in the perturbation theory, or else that we go to higher order in the perturbation theory, as a nonabelian and non-Euclidean extension of second-order wave-packet theory [63,64]. If such a system could be identified, then the physics of V_χ, which induces a Gross-Pitaevskii equation for the isospin, could be quite interesting. In the coupling between a wave packet and a rigid soliton, for instance, we see that this term produces at leading order a force proportional to $\dot{\chi}$. Thus, a change in the spin carried by the magnon produces a real-space force on the soliton. We leave the search for systems in which V_χ could produce significant effects to future research.

Finally, let us caution the reader that Eq. (27c) gives the dynamics of the isospin, which is defined with respect to the A and B sublattices, not with the laboratory frame. A right-handed mode, for instance, is by our definition always dominated by the A sublattice, which means that it carries opposite spin on either side of a domain wall. To return to the laboratory frame, one should apply the inverse rotation operator R^{-1} to the spin texture. To extract the laboratory-frame spin, then, lift R^{-1} to SU(2) by the standard homomorphism [65] and apply it to the isospin. The (semiclassical) spin

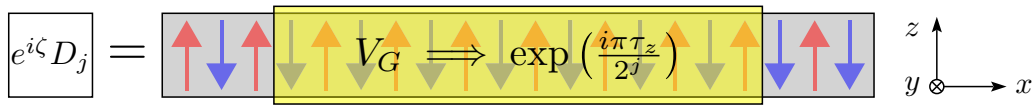

FIG. 4. The system under investigation in Sec. IV A. An in-plane easy-axis ($\hat{z}$) AFM is oriented in a nanostrip geometry, perpendicular to the easy axis ($\hat{x}$). A section of the sample is subjected to a gate voltage V_G applied normal to the sample plane, in the $\hat{y}$ direction. We show in Eq. (32) that the resulting isospin dynamics corresponds to a rotation about σ_z on the Bloch sphere (Fig. 2). We define here the notation $D_j = \mathrm{diag}(1, e^{i\pi/2^j})$, and is given by this applied DMI gate up to a dynamical phase $e^{i\zeta}$. Note, as a reference, that $\tau_z = D_0$.

carried at time t by the magnon with isospin $\boldsymbol{\eta}(t)$ is then [66]

$$|\boldsymbol{s}(t)\rangle = \begin{pmatrix} e^{i(\psi+\phi)}\cos\frac{\theta}{2} & e^{i(\psi-\phi)}\sin\frac{\theta}{2} \\ -e^{-i(\psi-\phi)}\sin\frac{\theta}{2} & e^{-i(\psi+\phi)}\cos\frac{\theta}{2} \end{pmatrix}|\boldsymbol{\eta}(t)\rangle, \quad (29)$$

where the Euler angles defining the texture are evaluated at $\mathbf{x}_c(t)$. The observable magnetization carried by the isospin is then $m_z = -\langle \boldsymbol{s}|\sigma_z|\boldsymbol{s}\rangle$, the sign arising from the fact that right-handed waves $|0\rangle$ carry negative spin. Since we are generally interested in systems with easy-axis anisotropy, the matrix transformation in Eq. (29) will typically result in a simple sign $m_z = \mp\langle\boldsymbol{\eta}|\sigma_z|\boldsymbol{\eta}\rangle$ depending on whether the local Néel order along the easy axis is pointing along $\pm\hat{z}$.

The key result of our wave-packet analysis, as regards the remainder of this paper, is that the isospin $\boldsymbol{\eta}$ obeys an emergent Schrödinger equation, and its dynamics is therefore governed by unitary time evolution. By tailoring our Hamiltonian, we can generate unitary rotations about multiple different axes in isospin space. We display a collection of different rotations in the coming examples, which taken together will be sufficient to generate any generic rotation (in three Euler angles) of the isospin.

IV. APPLICATION TO SELECTED MAGNONIC PRIMITIVES

In the previous section, we derived a set of semiclassical equations governing the isospin-coupled dynamics of a magnon wave packet. Now, we apply that formalism to two AFM magnonic systems: a gated 1D wire and a 1D domain wall. We conclude by mentioning the effects of magnetic fields and hard-axis anisotropy.

A. A gated AFM nanostrip: The magnon FET

In this section, we consider the application of a gate voltage across a one-dimensional (1D) AFM nanowire (extended along $\hat{x}$) with in-plane easy-axis anisotropy (along $\hat{z}$). The gate voltage breaks inversion symmetry, and will therefore generate a nonzero DMI simply by symmetry considerations [21]. In comparison to the DMI statically generated by inversion asymmetry due to interfacial or crystal structure effects, though, one expects the DMI produced by the gate to be tunable, and therefore a useful knob to access in a magnonic computing scheme. The system has been outlined schematically in Fig. 4.

Our motivation here is threefold. First, this gate will be extremely important in our device proposals later in the paper, so it is worthwhile to present the theoretical treatment here. Second, this simple example which does *not* possess any spin texture will provide a transparent presentation to demonstrate the general solution method to the reader. Finally, solving this problem, which has already been considered in the Néel vector picture, for the special case of linearly polarized waves, by Ref. [11], will serve as a validation of our theoretical methods against the literature.

The free energy has four parts: homogeneous and inhomogeneous exchange, easy-axis anisotropy, and DMI. The first three of these are the same as is given in Eqs. (1), and the DMI term is

$$F_{\mathrm{DMI}} = \frac{1}{2}\int \mathbf{D}\cdot[\mathbf{m}_A \times \partial_x \mathbf{m}_B + \mathbf{m}_B \times \partial_x \mathbf{m}_A]dx, \quad (30)$$

where $\mathbf{D} = D\hat{z}$. From the corresponding 4×4 Hamiltonian, we construct the 2×2 isospin Hamiltonian by using the embedding $E^\dagger$ and Eq. (25). Writing out $\mathscr{H} = \mathscr{H}_0 + \mathscr{H}_j\sigma_j$ explicitly for this problem, we find that it has an unimportant [67] constant part as well as a σ_z component:

$$\mathscr{H}_z = \frac{J|D|k\epsilon\left(1-\frac{(k\epsilon)^2}{2}\right)}{\hbar s\sqrt{2KJ+(Jk\epsilon)^2}}. \quad (31)$$

If we assume both that K/J is small and that k is in a regime where the distance between the split bands is constant in k, namely, well above the resonance frequency, then the denominator of Eq. (31) can be approximated merely by $\hbar s J k\epsilon$, canceling the linear contribution in the numerator and leaving only the constant term with a weak quadratic correction. Making these approximations in Eq. (31), we arrive at an isospin Hamiltonian

$$\mathscr{H}_z = D/S. \quad (32)$$

How does this Hamiltonian act on the isospin state? Since we are dealing with a Schrödinger equation [Eq. (27c)], we need only compute the unitary time evolution operator

$$U(t_1,t_0) = \exp\left[\frac{i\tau_z}{\hbar s}\int_{t_0}^{t_1} D\,dt\right] \quad (33)$$

$$= \exp\left[\frac{i\tau_z}{\hbar s}\left(\frac{\partial\omega}{\partial k}\right)^{-1}\int_{x_0}^{x_1} D\,dx\right]. \quad (34)$$

This is a rotation operator in isospin space, rotating about the $\hat{z}$ axis on the Bloch sphere by a total angle proportional to D and the length of the gate, but inversely proportional to the spin wave speed $\partial_k\omega$ and the spin magnitude S. The rate of rotation on the Bloch sphere works out to

$$\nabla\phi = \frac{1}{s}\frac{D}{J}. \quad (35)$$

Note that we have cited the rate of rotation on the Bloch sphere, where ϕ is the azimuthal angle: this differs by a factor

of 2 from the polarization angle of the staggered order. X- and Y-polarized states, which appear to be rotations of $\pi/2$ away from each other in the trace of a spin excitation, are actually π away from each other on the Bloch sphere (Fig. 2).

Because the rate of rotation scales with the DMI itself, the rotation on a single gate can be manipulated online simply by modulating the gate voltage. We concerned ourselves in Ref. [11] [with which our result in Eq. (32) agrees] mostly with a rotation between X and Y polarizations, but access to generic rotations will be crucial for a mature implementation of nonabelian magnonics.

B. Domain-wall retarder

Since applied AFM magnonics has become fashionable in the last decade, the AFM domain wall has undergone quite a bit of new analysis [12–14,16], and in decades past was a prototypical nontriviality for the AFM nonlinear sigma model [68–71]. Many such studies have concluded that spin waves passing through a domain wall experience a relative frequency shift between the right- and left-handed components [14]. In systems with DMI, they can express even more pronounced shifts between linearly polarized modes, giving rise to a retarding waveplate effect [12]. Our formalism allows us to calculate this shift precisely, and in terms of the SU(2) isospin.

In this section, we consider a Bloch-type domain wall in a synthetic AFM with easy-axis anisotropy and a bulk-type DMI. Take the Walker solution for the 1D texture as

$$\theta(x) = -2\arctan\left(\exp\frac{x}{\lambda}\right) \quad \text{and} \quad \phi(x) = -\pi/2, \tag{36}$$

with $\lambda = \sqrt{J/K} = O(\mathbb{A}^{-1})$ the domain-wall width.

With this texture, we can immediately calculate the texture-induced gauge fields from Eq. (B2) (taking $\psi = 0$ for concreteness): we have $\mathbf{A}^z = 0$ and

$$\mathbf{A}^x = \frac{1}{\lambda}\sin\psi\,\operatorname{sech}\frac{x}{\lambda} \tag{37a}$$

$$\text{and} \quad \mathbf{A}^y = \frac{1}{\lambda}\cos\psi\,\operatorname{sech}\frac{x}{\lambda} \tag{37b}$$

$$\Rightarrow \mathcal{A} = \frac{i}{\lambda\sqrt{2}}\operatorname{sech}\frac{x}{\lambda}, \tag{37c}$$

where we have suppressed the space-time index since there is only one [72]. The bulk-type DMI is written as $\mathbf{D}_{ij} = D\hat{r}_{ij}$, and minimization of DMI energy has been used to determine $\phi(x)$.

Using spin wave Hamiltonian $\mathcal{H}$ for synthetic AFMs detailed in the Supplemental Material [52], we compute the appropriate coefficients of the semiclassical dynamics in Eqs. (27). The resulting isospin Hamiltonian has an again unimportant $\mathbb{1}_2$ component as well as a τ_x component. The τ_x term is

$$\mathscr{H}_x = \frac{\mathcal{D}K(Z + 2Jk^2)}{4\ell\sqrt{JK}}\operatorname{sech}\frac{x}{\lambda}. \tag{38}$$

Since $\mathscr{H}$ has no other nontrivial component, we see immediately that it will carry out a rotation of the isospin about $\hat{x}$ on the Bloch sphere, and will do so most strongly near the center of the domain wall due to the exponential localization provided by $\operatorname{sech}(x/\lambda)$.

From there, we have $\mathcal{E}$ (since we have $\mathcal{H}$), $\mathscr{H}$ (since we have $\mathcal{H}$ and E), and we know that the $\mathbf{B} = \mathbf{E} = 0$ by inspection of $\mathbf{A}^z$. The other Berry curvature terms are easily seen to vanish as well. We immediately construct the semiclassical equations (27) and integrate them with an adaptive-step size Runge-Kutta-Fehlberg solver (`RKF45`), using the parameters for yttrium iron garnet to define our ferromagnetic layers [73]. Our results are displayed and discussed in Fig. 5. Note that, deep within the domain wall, the "easy axis" is no longer aligned with the textural slow mode, and the dispersion becomes imaginary for modes below a critical energy. In this case, spin transferred to the domain wall is the dominant process, and our numerical calculations break down close to this regime. Augmenting our theory with a collective coordinate theory of the domain wall, effectively allowing it to absorb spin, may be used to address this problem. Here, however, we keep the problem pedagogical by simply assuming that spin waves are sufficiently high energy that the local Hamiltonian remains Hermitian.

In our analysis of the domain-wall retarder, we note an important difference between the g-type and synthetic AFM in action. Define $\mathcal{C} = \sigma_x \otimes \mathbb{1}_2$, which exchanges each underlying basis field with its conjugate (time-reversed) partner. This operation corresponds to *charge conjugation*. $\mathcal{C}$ changes the sign of the coupling between spin wave and the emergent electromagnetic fields arising from spin texture and DMI. Together with time reversal (given by complex conjugation), the full chirality operator $\mathcal{S} = \mathcal{T}\mathcal{C}$ is a symmetry of the degenerate Néel-state Hamiltonian $\mathcal{H} = \hat{h} \oplus \hat{h}^*$. The breaking of $\mathcal{S}$ symmetry by spin texture in the domain wall is what allows the relative amplitudes of right- and left-handed modes to change in the overall wave function.

Now, define $\mathcal{I} = \mathbb{1}_2 \otimes \sigma_x$, which defines the sublattice interchange operation. $\mathcal{T}\mathcal{I}$ is also a symmetry of the degenerate Hamiltonian. In the g-type AFM case, spin texture will break $\mathcal{T}\mathcal{I}$ symmetry in general because an infinitesimal misalignment is present in each unit cell [28]. In the synthetic antiferromagnetic (SAF), however, the two sublattice sites in a unit cell are never misaligned, so that $\mathcal{T}\mathcal{I}$ is preserved even in the presence of spin texture.

Algebraically, the $\mathcal{T}\mathcal{I}$ symmetry of the SAF restricts off-block-diagonal terms of the 4×4 spin wave Hamiltonian to be purely real. Since the embedding E is itself real, it follows that the isospin Hamiltonian cannot have a nonzero τ_y component. The disentangling of $\mathcal{T}\mathcal{I}$ from $\mathcal{S}$ symmetry in SAFs should be seen as a virtue: it means that we can use SAFs to carry out rotations about precisely known axes. By contrast, the g-type calculation in Fig. 5 shows that symmetry-unconstrained rotations can be quite complex. Not only is the axis of rotation not about a canonical basis vector, but the axis of rotation *changes dynamically* as the wave packet travels through the continuum of different local Hamiltonians presented by the spin texture. Precise rotations appear to be insufferably difficult to control in such an AFM, so our prescription to experimentalists and device engineers is to use an SAF when precision is needed. However, SAFs present their own challenges. Unlike pure g-type AFMs, SAFs present a shape anisotropy that may make the realization of uniaxial

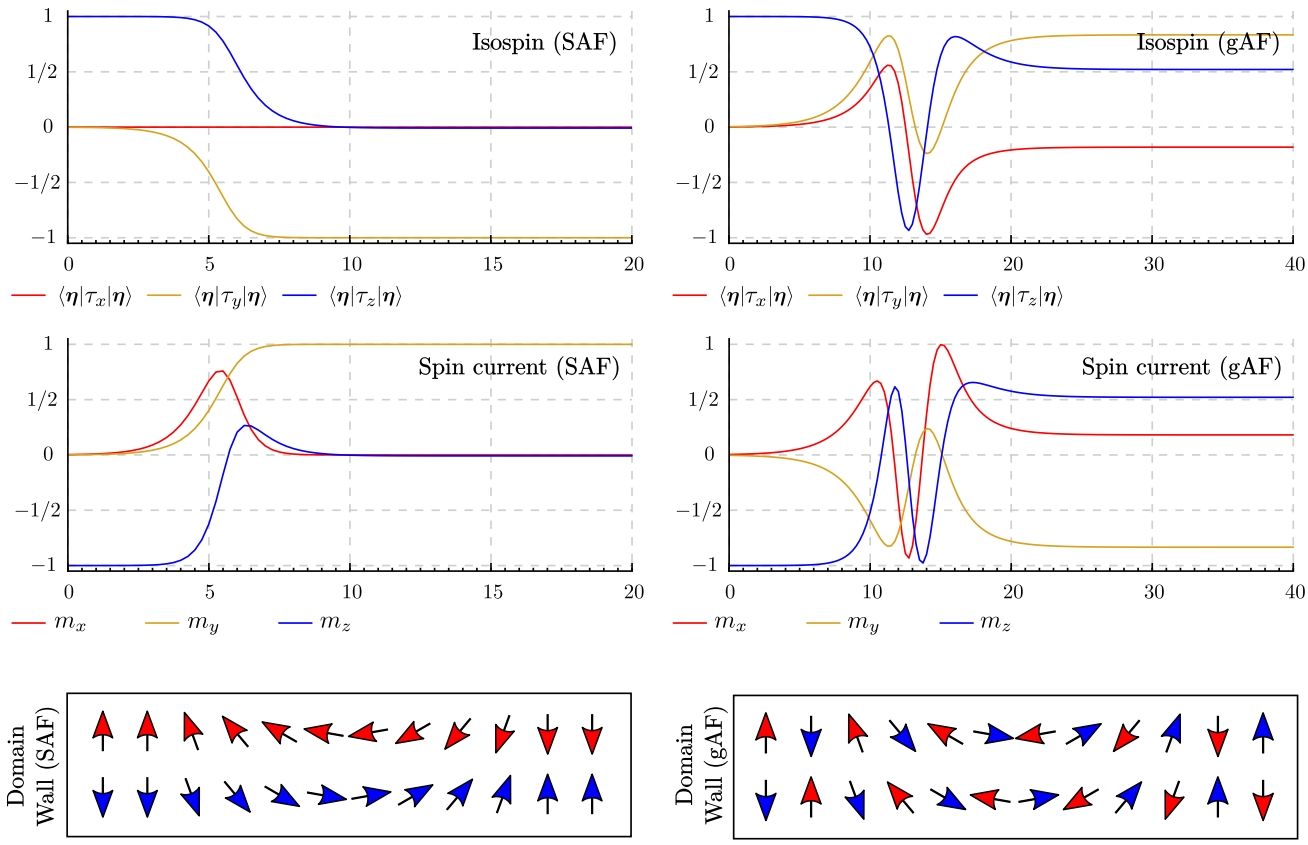

FIG. 5. Semiclassical dynamics of a single magnon passing through a Bloch-type domain wall. The horizontal axes represent time, given in picoseconds. Left: integration of Eqs. (27) for a wave packet, initially with right-handed polarization $\boldsymbol{\eta} = |0\rangle$, passing through a domain wall in a synthetic AFM. The SAF material parameters were taken from YIG, and the initial frequency of the wave packet was tuned to result in a $\pi/2$ rotation on the Bloch sphere. The top plot gives the isospin expectation values; bottom, these have been rotated to give the true spin current. Right: the same semiclassical dynamics, domain wall, and YIG parameters are simulated, but the system is assumed to be g-type AFM. We merely substitute the ferromagnetic exchange for the inhomogeneous exchange, and antiferromagnetic for homogeneous exchange. Because $\mathcal{TI}$ symmetry is broken in the g-type configuration, the rotation is unavoidably more complex. Bottom: schematic illustration of a g-type versus a synthetic AFM domain wall. We have illustrated Néel-type walls for simplicity, but the calculation was done for Bloch-type walls.

perpendicular magnetic anisotropy (PMA) difficult to maintain. A possible solution would be to use a-type AFMs. These materials are magnetically ordered at the lattice level, but are AFM ordered in layers, rather than by nearest neighbors. These may present the best of both worlds: their symmetry constraints will disentangle different rotations, as with an SAF, but they would avoid shape anisotropy issues. Further materials research in this direction is warranted.

We emphasize that although our wave-packet theory describes a single semiclassical particle, it nonetheless applies to a global spin wave state [74]. Our results for both the domain wall and the magnon field effect transistor (FET) match the micromagnetic simulations of Refs. [12] and [11] to within 5% error in the driving frequency [75]. Formally, the global wave function can be decomposed usefully into wave packets through a Gabor transformation. Standard signal analysis indicates that this use of isospin wave packets as a basis for the spin wave signal is accurate as long as the grid spacing needed to sample the spatially inhomogeneous texture does not exceed the spread of wavelengths under consideration: $\Delta x_c \Delta k_c \leqslant 2\pi$.

C. Other gates

We have carried out explicit example calculations in the previous sections because they can be immediately compared to results in the literature, unifying these previous investigations under a single formalism and allowing the reader to put our results in context.

However, our formalism is far reaching and several other gates can be readily designed. From straightforward calculations of $\mathcal{H}$ and $\mathscr{H}$, one sees that a hard-axis anisotropy will provide a rotation about σ_x [76]. Note that this actually implies spin nonconservation since the magnetization (relative to the local quantization axis) carried by a spin wave corresponds to the polar angle of its isospin. Such nonconservation mechanisms have been explored elsewhere [77]; here we merely accept that they fall out of the isospin dynamical equations. Meanwhile, an applied magnetic field parallel with the AFM order will provide a rotation about σ_z since it breaks the chiral degeneracy but not the U(1) symmetry of the ground state. In this way, a parallel **B** field gives the same effect as a normal **E** field used to generate the DMI in Sec. IV A.

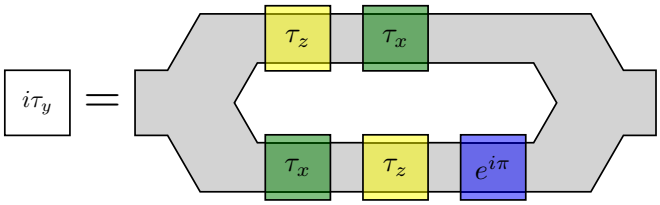

FIG. 6. Applying different unitary gates to different branches of a spin wave signal makes the entire Lie algebra of rotational generators available from a set of two, as in the generation of σ_y from the known σ_x and σ_z gates in the figure. By applying σ_x on one branch and σ_z on another, one could for instance generate a Hadamard gate. Note that in such a Hadamard gate, the designer must take care to ensure that the overall dynamical phase between the branches is equivalent, so as to avoid wave interference in the output channel. Since the U(1) phase is abelian, though, one need not worry about this in the $i\tau_y$ gate pictured above. Using a $D_1 = -i\tau_z$ gate instead of a pure τ_z gate would generate the same, "extraneous" $\pi/2$ phase on both branches.

A local modification of the easy-axis anisotropy can raise or lower the local AFMR frequency, and can therefore be used to adjust the relative U(1) phase between two spin wave arms of a multichannel magnonic signal. For instance, such a modification could be used to generate the blue $e^{i\pi}$ gate in Fig. 6. There, the sign provided by the U(1) relative phase is crucial for computing the commutator, rather than the anticommutator, of σ_x and σ_z, without the $e^{i\pi}$ gate, the loop in Fig. 6 would simply produce total destructive interference, annihilating the input signal. If one could implement this in a gate-controlled, switchable fashion, then electronic control over the $e^{i\pi}$ gate (EAA) and the σ_z gate (DMI) would turn Fig. 6 into a switchable $\sigma_x \leftrightarrow \sigma_y$ gate. The presence of an $e^{i\pi}$ gate allows multichannel schemes such as Fig. 6 to explore the full Lie algebra structure of SU(2). Options for implementing a switchable $e^{i\pi}$ gate could include gate-controlled easy-axis anisotropy or a perpendicular (to $\mathbf{n}$) applied $\mathbf{B}$ field. An especially important use of this gate in a isospin computer would be to compensate the accidental dynamical phase accumulated during the execution of rotational gates.

If one is interested in investigating the effects of interactions not considered here, one can simply derive the spin wave Hamiltonian in the four-dimensional basis we have used in this paper and then project it to the operator space over the degenerate subspace. One immediately obtains the corresponding isospin Hamiltonian. We have tried to cover the main classes of interactions in the Supplemental Material [52] but more unique interactions such as compass anisotropy [78] or honeycomb DMI [18] could provide useful interfaces to other isospin operations.

V. DISCUSSION

Our objective to this point has been to present the reader with a cohesive program for isospin magnonics. We started by reviewing the idea of chirality and the isospin vector that parametrizes it. Our key foundational results were the semiclassical equations (27) describing the isospin dynamics of an AFM magnonic wave packet. With these equations in hand, we described a collection of physical gates, with a focus on voltage gates and domain walls, that could manipulate the isospin in predictable, calculatable ways.

As this paper draws to a close, let us reflect on our results and potential avenues for future research. From the computing standpoint, recognition of the chiral degree of freedom in AFM magnons is of paramount importance. Using the isospin vector as a data carrier represents a paradigmatic improvement, on multiple fronts, over the amplitude-modulating proposals that permeate FM magnonics. First, power management and energy efficiency concerns that arise when information is encoded in the FM spin wave power spectrum become immaterial when the data are carried by AFM isospin. Many of the problems of architecture scaling, which plague FM magnonic computing, are significantly alleviated in AFMs. Second, the isospin carries a higher dimensionality of information. We have seen that this considerably broadens the scope of magnon algorithmics. For instance, it may be possible to replicate semiclassical quantum computing gates in isospin logic. If one is willing to accept the use of $2N$ isospin signals in place of 2^N qubits, and can map between these schemes faithfully, then perhaps one can "classically simulate" nonentangling quantum circuits on a classical magnonic platform. To this end, a great deal of study is needed here to properly characterize the power and scope of isospin computing.

Our key contribution to the field of magnonics is the development of a generic, unified formalism for describing the isospin dynamics in terms of unitary time evolution, a framework with which every physicist is intimately familiar. Together with our mechanical recipe (A10) for generating the isospin Hamiltonian from the free energy, we expect that our theory provides a cohesive platform for future theoretical and experimental investigations into the challenges of isospin magnonics.

Among these challenges are both extensions and applications of our theoretical apparatus. The gates we investigated in Sec. IV were purely one dimensional, and from these simple components one can produce quite sophisticated computing devices. We have taken pains, however, to keep the spatial dimensionality of our theory generic; one can apply the results of this paper to 2D and 3D systems. Even in quasi-1D magnetic strips, two-dimensional textures such as skyrmions or magnetic vortices could produce interesting effects. The interactions between such solitons and AFM spin waves in open systems is also an open question. Our theory could be used to address these issues.

There of course exist magnonic applications outside the spin wave approximation that underlie the theory in this paper. There, our technical theory may not be a suitable tool, but we hope that our phenomenological description of the SU(2) isospin, a concept which relies solely on a the fact that there are two sublattice degrees of freedom with a relative phase between them, will prove useful. Recently, for instance, AFM auto-oscillators have been proposed [79,80]. The dynamical differences between AFM and FM (Klein-Gordon versus Schrödinger) suggest that existing theories of magnetic auto-oscillation [81] will need to be extended for the AFM case. This has already been done in the case of easy-plane oscillators, where the magnetization produced

by an oscillation is relatively fixed [82]. Other second-order oscillator theories exist, but, especially once they become coupled, are often intractable [83,84]. They are also usually considered as phase oscillators. Whether these are the most natural theories for describing isospin oscillators is an open question.

In the AFM case, for instance, will the concept of an auto-oscillation bandwidth extend to neighborhoods on the isospin Bloch sphere? Such questions, which inherently depend on nonlinearity, call for an understanding of isospin beyond the harmonic spin wave regime. Along a different direction, the adventurous theorist might consider extending our theory to an AFM of more than two sublattices, attempting to derive the dynamics of an SU(N) isospin.

Practical questions remain about the classes of materials that can reliably support the sort of dynamics we have espoused in this paper. Although our theory readily applies to uniaxial AFMs such as MnF_2, AFMs with biaxial or multiaxial anisotropy may not support low-lying circularly polarized modes. Circularly polarized modes may still be used as a basis, especially if the second anisotropy axis is weak, but as the band splitting becomes greater and greater, our "nearly degenerate" assumption breaks down. More thorough work is needed in understanding isospin dynamics in this regime [77].

Finally, we note that ferrimagnets satisfy conceptual prerequisites for an SU(2) isospin, but are usually treated [in the yttrium iron garnet (YIG) case, at least] merely as low-damping FMs. Given the importance of ferrimagnets to modern magnonics, a theoretical extension of our formalism to these systems could be of immense interest. Although the two modes in ferrimagnets would not be degenerate as they are in AFMs, and therefore would require more energy for switching, one might still in principle be able to carry out isospin logical operations. Research into such systems could be critical for applied isospin computing.

ACKNOWLEDGMENTS

We gratefully acknowledge X. Wu, Y. Gao, J. Lan, V. Siddhu, and Z. McDargh for our insightful conversations. This work was supported by the National Science Foundation (NSF), Office of Emerging Frontiers in Research and Innovation, under Award No. EFRI-1433496 (M.W.D.), the NSF East Asia and Pacific Summer Institute under Award No. EAPSI-1515121 (M.W.D.), and the National Natural Science Foundation of China under Grants No. 11722430 and No. 11474065 (W.Y. and J.X.).

APPENDIX A: TEMPORAL DYNAMICS FROM THE BERRY PHASE LAGRANGIAN

Although we introduced spin wave dynamics via Eq. (4), it is possible to bypass the Landau-Lifshitz equation altogether. Instead, we can appeal directly to the Lagrangian of our classical field theory on $\alpha_p m$ and $\beta_\pm$, given by

$$L[\alpha_+, \beta_+, \alpha_-, \beta_-] = L^{\mathrm{BP}} - F, \tag{A1}$$

where F is the magnetic free energy and L^{BP} is the so-called Berry phase Lagrangian. The Berry phase Lagrangian is given by

$$L^{\mathrm{BP}} = \frac{S}{\epsilon^d} \sum_{\Gamma}^{A,B} \int \frac{\mathbf{\Omega}_\Gamma \times \mathbf{m}_\Gamma}{1 - \mathbf{\Omega}_\Gamma} \cdot \frac{d\mathbf{m}_\Gamma}{dt}\, d^d x, \tag{A2}$$

where ϵ is the lattice constant and $\mathbf{\Omega}$ is the gauge-dependent orientation of the local Dirac string [85–87]. If one takes the variational derivative of L^{BP} by α and β, we will find the left-hand side of Eq. (5). Even though we have already arrived at this result from the perspective of the Landau-Lifshitz equation, we repeat the derivation here using the Lagrangian picture. We do so because the Lagrangian formalism should be of greater generality and modularity [88], so that others may simply add terms to the Lagrangian and repeat the process we are about to demonstrate.

Define $\lambda_A = \sqrt{1 - 2|\alpha|^2}$, $\lambda_B = \sqrt{1 - 2|\beta|^2}$, and $\lambda_m = \sqrt{1 - 2|\mu|^2}$ (we use the convention that $|\alpha|^2 = \alpha_+\alpha_-$ and so on). The basic idea in evaluating L^{BP} is simply to make the substitutions

$$\begin{aligned} R\mathbf{m}_A = {} & \frac{\hat{x}}{\sqrt{2}}[\alpha_+ + \alpha_- + \lambda_A(\mu + \mu^*)] \\ & + \frac{\hat{y}}{i\sqrt{2}}[\alpha_+ - \alpha_- + \lambda_A(\mu - \mu^*)] \\ & + \hat{z}(\lambda_A\lambda_m - \alpha_-\mu - \mu^*\alpha_+), \end{aligned} \tag{A3a}$$

$$\begin{aligned} R\mathbf{m}_B = {} & \frac{\hat{x}}{\sqrt{2}}[\beta_+ + \beta_- + \lambda_B(\mu + \mu^*)] \\ & + \frac{\hat{y}}{i\sqrt{2}}[\beta_+ - \beta_- + \lambda_B(\mu - \mu^*)] \\ & - \hat{z}(\lambda_B\lambda_m - \beta_-\mu - \mu^*\beta_+) \end{aligned} \tag{A3b}$$

into the Lagrangian and expand the result. The "monolithic substitutions" (A3) are derived in Appendix C. As long as the Lagrangian is a linear operator on the spin wave fields $\alpha_\pm$ and $\beta_\pm$, we end up with a collection of terms

$$L^{\mathrm{BP}} = L_0^{\mathrm{BP}} + L_1^{\mathrm{BP}} + L_2^{\mathrm{BP}}, \tag{A4}$$

where we have collected terms at zeroth, linear, and quadratic order in the spin wave fields. Linear spin wave theory, upon which our formalism is built, cannot support terms at cubic order or higher, as these would constitute nonlinearities in the equations of motion.

Because we are interested in taking functional derivatives with respect to the spin wave fields, we can immediately neglect the terms L_0^{BP} [89]. As for L_1^{BP}, we see that functional derivatives of this term would actually introduce inhomogeneous terms in the equations of motion. The fastidious reader will find in her derivations that we apparently *do* have such terms in our Lagrangian, which do not vanish *a priori*. Such terms, if they properly belong to a physical description of the system, would seem to imply spontaneous emission of spin waves since they will let $\dot{\Psi}$ take on a nonzero value even when Ψ is everywhere zero.

However, the reader is simultaneously invited to notice that we have introduced more "perturbations" than we can actually control. The problem is that $\mathbb{A}$, which we treat as an independent field, encodes the ground state of the system, as predetermined by anisotropy and DMI. In fact, once the

boundary conditions are given, $\mathbb{A}$ is strictly determined by these parameters [90]. In equilibrium, one may compute $\mathbb{A}$ in principle by minimizing the free-energy functional with respect to the textural gauge fields

$$\left\{\frac{\delta F[\mathbf{D}, K]}{\partial A_\mu^j} = 0\right\}_{\mu,j} \Rightarrow \mathbb{A}_{\text{equilibrium}}[\mathbf{D}, K]. \tag{A5}$$

Formally, these equations should be solved simultaneously with the actual spin wave equation. On physical grounds, though, we assume that these inhomogeneous terms always vanish when the system under consideration is in equilibrium or else, the system would not in equilibrium, leading to a contradiction. The mathematical mechanism transmitting this assumption is precisely the set of constraints (A5). If the system is not in equilibrium, say, if a soliton is moving, then generally speaking it should generate spin waves inhomogeneously. Although our formalism allows for temporal behavior of the underlying spin texture, we assume that it is always in *quasistatic equilibrium*, that is, we neglect any inhomogeneous spin waves it generates.

After the above considerations are implemented, we find that we need deal only with the harmonic Lagrangian

$$L^{\text{BP}} \mapsto L_2^{\text{BP}}. \tag{A6}$$

Keeping only the quadratic terms in the spin wave modes, keeping terms only to order $O(|\mathbb{A}|^2)$ in our perturbative expansion, and summing over the sublattices $\Gamma \in \{A, B\}$, we are left merely with

$$L_2^{\text{BP}} = S\left[A_t^z \alpha_- \alpha_+ + \frac{in}{2}(\alpha_- \dot{\alpha}_+ - \alpha_+ \dot{\alpha}_-)\right] - S\left[A_t^z \beta_- \beta_+ + \frac{in}{2}(\beta_- \dot{\beta}_+ - \beta_+ \dot{\beta}_-)\right], \tag{A7}$$

where $n = 1 + |\mu|^2$ is the effective index of refraction between the local and vacuum values of the spin wave speed, as seen from the Klein-Gordon formulation (see Appendix E). One readily observes the difference of a minus sign separating sublattices A and B, as well as a minus sign between each field and its conjugate partner. These signs are precisely our $\tau_z \otimes \sigma_z$ factor from Eq. (5). Defining $\Psi = (\alpha_+, \beta_+, \alpha_-, \beta_-)$, we find that setting $\delta L/\delta \bar{\Psi} = 0$ results in

$$i(\tau_z \otimes \sigma_z)\dot{\Psi} = \frac{\epsilon^d}{nS}\frac{\delta F}{\delta \bar{\Psi}} - A_t^z(\mathbb{1}_2 \otimes \sigma_z)\Psi, \tag{A8}$$

where ϵ is the lattice constant. Since we will only keep the quadratic terms in F by the arguments that lead to Eq. (A6), we know that $\delta F/\delta \Psi^*$ is a linear operation on Ψ that can be written in the form

$$i(\tau_z \otimes \sigma_z)\dot{\Psi} = \frac{\epsilon^d}{nS}\mathcal{H}\Psi - A_t^z(\mathbb{1}_2 \otimes \sigma_z)\Psi \tag{A9}$$

analogous to Eq. (5). In general, the spin wave Hamiltonian is given by

$$\mathcal{H} = \begin{pmatrix} \left\langle \frac{\delta F}{\partial \alpha_-}\middle|\alpha_+\right\rangle & \left\langle \frac{\delta F}{\partial \alpha_-}\middle|\beta_+\right\rangle & \left\langle \frac{\delta F}{\partial \alpha_-}\middle|\alpha_-\right\rangle & \left\langle \frac{\delta F}{\partial \alpha_-}\middle|\beta_-\right\rangle \\ \left\langle \frac{\delta F}{\partial \beta_-}\middle|\alpha_+\right\rangle & \left\langle \frac{\delta F}{\partial \beta_-}\middle|\beta_+\right\rangle & \left\langle \frac{\delta F}{\partial \beta_-}\middle|\alpha_-\right\rangle & \left\langle \frac{\delta F}{\partial \beta_-}\middle|\beta_-\right\rangle \\ \left\langle \frac{\delta F}{\partial \alpha_+}\middle|\alpha_+\right\rangle & \left\langle \frac{\delta F}{\partial \alpha_+}\middle|\beta_+\right\rangle & \left\langle \frac{\delta F}{\partial \alpha_+}\middle|\alpha_-\right\rangle & \left\langle \frac{\delta F}{\partial \alpha_+}\middle|\beta_-\right\rangle \\ \left\langle \frac{\delta F}{\partial \beta_+}\middle|\alpha_+\right\rangle & \left\langle \frac{\delta F}{\partial \beta_+}\middle|\beta_+\right\rangle & \left\langle \frac{\delta F}{\partial \beta_+}\middle|\alpha_-\right\rangle & \left\langle \frac{\delta F}{\partial \beta_+}\middle|\beta_-\right\rangle \end{pmatrix}, \tag{A10}$$

where the bra-ket notation simply indicates a functional inner product under which the basis vectors corresponding to $\alpha_\pm$ and $\beta_\pm$ are orthogonal. Since the formula we have given for $\mathcal{H}$ is explicit and straightforward [just make the substitutions (A3) into the free energy and start taking functional derivatives of the quadratic sector], we will not bore the reader with pages of algebra by deriving concrete manifestations of $\mathcal{H}$ in the main text. We have provided computer algebra code (in the Wolfram language) that derives $\mathcal{H}$ for an assortment of useful free energies in the Supplemental Material [52], with a focus on those free energies needed to explore our various examples in Sec. IV. We hope readers interested in their own systems will use the recipe described above to generate their own spin wave Hamiltonians, which project onto a Hamiltonian $\mathscr{H}$ governing the unitary dynamics of the isospin vector $|\boldsymbol{\eta}\rangle$ in Sec. III.

APPENDIX B: SPIN TEXTURE

A principal mechanism [91] by which we break U(1) symmetry and mix the chiralities is through the introduction of a nonuniform ground state. To that end, we require a formal structure for encoding information about the ground state in our dynamical equations.

Much of the contemporary literature dealing with spin texture opts to assemble a local coordinate frame, generally $\{\hat{e}_r, \hat{e}_\theta, \hat{e}_\phi\}$, so that the linearization process we used to derive Eq. (6) can be recycled in the $\{\hat{e}_\theta, \hat{e}_\phi\}$ plane. This amounts to a passive transformation, taking the oscillatory plane of the spin wave fluctuations to align with the local texture.

We instead opt to carry out the equivalent *active transformation*, rotating each spin so that its spin wave plane coincides with the global xy plane [34,35,44]. A thorough introduction to this technique in the ferromagnetic case is given by Ref. [34]. In ferromagnets, one simply defines a rotation matrix $\hat{R}(\mathbf{x}, t)$ by $\hat{R}\mathbf{m}^0 = \hat{z}$, so that it sends the ground-state configuration $\mathbf{m}(\mathbf{x}, t)$ at each point to the global $\hat{z}$ axis. This rotation matrix gives rise to a gauge field $\mathbb{A}_\mu = (\partial_\mu \hat{R})\hat{R}^T$. Formally, ω may be regarded as a matrix-valued [SO(3)-valued] one-form.

One can show in the lattice formalism that $\mathbb{A}$ represents the infinitesimal rotation $1 + R_i R_j^T = \exp \mathbb{A}_{ij}$ between two sites, that is, $\mathbb{A}$ is a generator of rotations. It can thus be decomposed into the standard basis for SO(3):

$$\mathbb{A}_\mu = A_\mu^x \hat{J}_x + A_\mu^y \hat{J}_y + A_\mu^z \hat{J}_z. \tag{B1}$$

Defining R in terms of the Euler angles $R = e^{-i\psi \hat{J}_z} e^{-i\theta \hat{J}_y} e^{-i\phi \hat{J}_z}$, we can express the vector fields $\mathbf{A}^j$ in terms of the spherical angles describing the spin texture. This is why we have chosen to include minus signs in the exponentials defining R: they show that we first "undo" the spherical angles by sending the azimuth to $\phi - \phi = 0$ and then sending the polar angle to zero. Taking this convention gives us

$$A_\mu^x = -\sin\psi\, \partial_\mu\theta + \cos\phi \sin\theta\, \partial_\mu\phi, \tag{B2a}$$

$$A_\mu^y = -\cos\psi\, \partial_\mu\theta - \sin\theta \sin\psi\, \partial_\mu\phi, \tag{B2b}$$

$$A_\mu^z = -\cos\theta\, \partial_\mu\phi - \partial_\mu\psi. \tag{B2c}$$

Since only two angles are needed to specify the state of each spin, the third rotation by ψ appears to by extraneous, though certainly permitted since it leaves invariant the spin texture now lying along $\hat{z}$. In this sense, it represent the U(1) gauge freedom associated with the U(1) symmetry of a coherent spin. In practice, though, ψ will often *not* be a gauge freedom because the U(1) symmetry will often be broken by means other than the immediate spin texture. If the spin texture has any misalignment with the easy axis, that is, if there is *any* deviation from the Néel ground state, then the anisotropy energy will not be invariant under the rotation by ψ. DMI or hard-axis anisotropy vectors lying perpendicular to the ground state would also break this symmetry.

The fact that we have chosen $\hat{z}$ as the global axis to which the texture is rotated means that we will mostly be concerned with the J_z component of the curvature form $\mathbf{\Omega} = \mathrm{d}\mathbb{A}$. The main consequence is that it is the curl of $\mathbf{A}^z$, rather than the curl of $\mathbf{A}^x$ or $\mathbf{A}^y$, which will provide the emergent electromagnetic field, familiar to students of magnetic skyrmions [62], generated by a spin texture.

The reader may recall that $\mathbb{A}$, and therefore the 3-tuple $(\mathbf{A}^x, \mathbf{A}^y, \mathbf{A}^z)$, was supposed to describe an infinitesimal rotation between neighboring spins. Such a rotation belongs to a two-dimensional group, and should be describable by exactly two numbers; therefore, we should seek a single constraint among our three vector potentials $\mathbf{A}^j$. By analyzing the curvature form, one can quickly show that this constraint is

$$\nabla \times \mathbf{A}^z = \mathbf{A}^x \times \mathbf{A}^y. \tag{B3}$$

Because $\hat{z}$ is privileged, it will be convenient to keep using $\mathbf{A}^z$ in our equations. For $\mathbf{A}^x$ and $\mathbf{A}^y$, though, we define a more concise complex field via

$$\mathcal{A}_\mu = \frac{A^x_\mu + i A^y_\mu}{\sqrt{2}}. \tag{B4}$$

Then, we see that we can substitute the right-hand side of Eq. (B3) for [92]

$$\hat{z} \cdot (\mathbf{A}^x \times \mathbf{A}^y) = A^x_x A^y_y - A^x_y A^y_x = 2i\mathcal{A}^*_x \mathcal{A}_y. \tag{B5}$$

We conclude that $\mathcal{A}^*_x \mathcal{A}_y$, and, therefore, $\mathcal{A}^*_y \mathcal{A}_x$, is a physically interesting quantity, as it encodes the same emergent electromagnetic field as the curl of $\mathbf{A}^z$.

What of the symmetric products $\mathcal{A}^*_\mu \mathcal{A}_\mu$? It turns out that these elements are also gauge-invariant physical quantities. In the general case, one finds

$$\mathcal{A}^*_\mu \mathcal{A}_\nu = g_{\mu\nu} + \frac{i}{2} F_{\mu\nu}, \tag{B6}$$

$$\text{defining} \quad Q_{\mu\nu} = \mathcal{A}_\mu \mathcal{A}^*_\nu, \tag{B7}$$

where $g_{\mu\nu} = A^x_\mu A^x_\nu + A^y_\mu A^y_\nu$ reduces in spherical angles of the texture to

$$g_{\mu\nu} = \partial_\mu\theta\partial_\mu\theta + \sin^2\theta\partial_\mu\phi\partial_\nu\phi \tag{B8}$$

$$\Rightarrow g = d\theta^2 + \sin^2\theta\, d\phi^2. \tag{B9}$$

In other words, g is just the first fundamental form on the sphere. It is the differential line element ds^2 by which arc lengths of the spin texture through spin space are measured. The matrix g is the spherical metric.

$Q_{\mu\nu}$ is called the *quantum geometric tensor*. There is very little "quantum" about it in our case, but the nomenclature is already out there [10,93–95].

APPENDIX C: A MONOLITHIC SUBSTITUTION FOR INTRODUCING THE SPIN WAVE FIELDS

In the antiferromagnetic case, we choose the rotation matrix to send the staggered order to the global $\hat{z}$. Generally speaking, $\mathbf{m}_A$ and $\mathbf{m}_B$ are not perfectly antiparallel, so after this rotation we will still be left with in-plane components of the (rotated) local magnetization.

We have already alluded to the fact that our two-level system does not fully describe the spin wave dynamics. This is because the basis fields $a_x + ia_y$ and $b_x + ib_y$ only represent circular modes. If we want to access modes with linear components, say, fluctuations of a_x with $a_y = 0$, then our Hamiltonian needs to couple to a linear combination of both $a_x + ia_y$ and its complex conjugate.

To address this, we have introduced the fields α_+, α_-, β_+, and β_- to represent our spin wave fluctuations on each sublattice. Now, let us fold these new variables into our formalism. First, split each rotated field into its slow ($\tilde{\mathbf{m}}^0_A$ and $\tilde{\mathbf{m}}^0_B$) and fast ($\boldsymbol{\alpha}$ and $\boldsymbol{\beta}$) modes, which are perpendicular by construction, and then split the slow modes into the local staggered order and local magnetization ($R\mathbf{n} = \lambda_m\hat{z}$ and $\tilde{\mathbf{m}} = R\mathbf{m}$, with $\lambda_m = \sqrt{1-m^2}$) of the quasistatic equilibrium spin texture. We have introduced factors of $\lambda_A = \sqrt{1-|\boldsymbol{\alpha}|^2}$ and $\lambda_B = \sqrt{1-|\boldsymbol{\beta}|^2}$ in order to maintain the normalization of the slow modes $\tilde{\mathbf{m}}_A$ and $\tilde{\mathbf{m}}_B$ in the presence of spin wave fluctuations. In other words, we have

$$R\mathbf{m}_A = \lambda_A(\tilde{\mathbf{m}} + \lambda_m\hat{z}) + \boldsymbol{\alpha}, \tag{C1a}$$

$$R\mathbf{m}_B = \lambda_B(\tilde{\mathbf{m}} - \lambda_m\hat{z}) + \boldsymbol{\beta}. \tag{C1b}$$

A few notes about the quantities we have just defined. First, $\tilde{\mathbf{m}}$ lies in the xy plane since $\tilde{\mathbf{n}} = \lambda_m\hat{z}$ is perfectly out of plane. Second, though we have opted out of a concern for brevity not to decorate $\mathbf{n}$ and $\mathbf{m}$ with any kind of indicator, keep in mind that these variables *only* encode the slow modes of the system. All spin wave fluctuations of these quantities have been restricted by construction to the excitations $\boldsymbol{\alpha}$ and $\boldsymbol{\beta}$.

Notice that we have chosen R through the realignment of $\mathbf{n}$ to avoid choosing a preferred sublattice. Because each $\mathbf{m}^0_A$ and $\mathbf{m}^0_B$ is subtly misaligned from $\mathbf{n}$ in the presence of a texture, however, our rotated spin wave fluctuations are $\boldsymbol{\alpha}$ and $\boldsymbol{\beta}$ have small out-of-plane components. It would be convenient instead to restrict them to the xy plane, so let us now compute exactly what their out-of-plane component is. Since they are orthogonal to the sublattice slow modes by construction, we have (on the A sublattice, for instance)

$$0 = \boldsymbol{\alpha} \cdot \tilde{\mathbf{m}}^0_A = \boldsymbol{\alpha} \cdot \tilde{\mathbf{m}} + \lambda_m\alpha_z \tag{C2}$$

so that $\alpha_z = -\lambda_m^{-1}\boldsymbol{\alpha} \cdot \tilde{\mathbf{m}}$ and $\beta_z = \lambda_m^{-1}\boldsymbol{\beta} \cdot \tilde{\mathbf{m}}$. Defining $\mathbf{a}$ and $\mathbf{b}$ as the planar projections of the spin wave fields, we can then simply write $\boldsymbol{\alpha} = \mathbf{a} - \lambda_m^{-1}(\mathbf{a} \cdot \tilde{\mathbf{m}})\hat{z}$ and so on.

Finally, we define complex variables $\alpha_\pm = (a_x \pm i a_y)/\sqrt{2}$, $\beta_\pm = (b_x \pm i b_y)/\sqrt{2}$, and $\mu = (\tilde{m}_x + i\tilde{m}_y)/\sqrt{2}$. These four complex variables will be treated as independent; with the understanding that the real part must be taken before extracting physical quantities from this complex formalism, four real degrees of freedom are maintained. Taking all of these definitions together, we have our two monolithic substitutions

$$\begin{aligned}\tilde{\mathbf{m}}_A = &\frac{\hat{x}}{\sqrt{2}}[\alpha_+ + \alpha_- + \lambda_A(\mu + \mu^*)] \\ &+ \frac{\hat{y}}{i\sqrt{2}}[\alpha_+ - \alpha_- + \lambda_A(\mu - \mu^*)] \\ &+ \hat{z}(\lambda_A\lambda_m - \alpha_-\mu - \mu^*\alpha_+), \end{aligned} \tag{C3a}$$

$$\begin{aligned}\tilde{\mathbf{m}}_B = &\frac{\hat{x}}{\sqrt{2}}[\beta_+ + \beta_- + \lambda_B(\mu + \mu^*)] \\ &+ \frac{\hat{y}}{i\sqrt{2}}[\beta_+ - \beta_- + \lambda_B(\mu - \mu^*)] \\ &- \hat{z}(\lambda_B\lambda_m - \beta_-\mu - \mu^*\beta_+). \end{aligned} \tag{C3b}$$

With these quantities in hand, the free energy can be computed explicitly, and by taking variations by α and β of the consequent Lagrangian, we can ultimately determine the spin wave equation of motion.

APPENDIX D: A MORE DETAILED DISCUSSION OF NONABELIAN WAVE-PACKET THEORY

Before computing a phase-space Lagrangian governing the semiclassical dynamics, we establish some self-consistency properties of the wave packet that will provide for useful identities during our calculation.

1. Normalization condition

First, let us enforce a normalization condition on $|W\rangle$, given by

$$\langle W|\tau_z \otimes \sigma_z|W\rangle = 1. \tag{D1}$$

This leads to a normalization condition for the η, namely, that

$$\langle W|\tau_z\sigma_z|W\rangle = (-1)^j \int d\mathbf{q}\, d\mathbf{k}\, w_k^* w_q \eta_{j,k}^* \eta_{j,q} \langle \psi_k^j|\sigma_z|\psi_q^j\rangle \tag{D2}$$

$$= (-1)^{2j} \int d\mathbf{q}\, |w_q|^2 |\eta_j|^2 \tag{D3}$$

$$\Rightarrow 1 = \langle \boldsymbol{\eta}|\boldsymbol{\eta}\rangle. \tag{D4}$$

Equation (D4) suggests that, unlike $|W\rangle$ and $|\Psi\rangle$, $|\boldsymbol{\eta}\rangle$ will be subject to a traditional, Euclidean Schrödinger dynamics. Recall that the σ_z inner product in the two-level system did not provide a useful normalization condition, as a result of the internal hyperbolic geometry. It is only here in the four-level system, where the signs from internal and external geometries cancel each other, that we arrive at a normalizable spin wave density (rather than spin density).

The calculational patterns from Eq. (D2) detail the internal derivations of wave-packet theory. We briefly outline the logical flow of the computation for readers unfamiliar with the formalism. The key stages needed to reduce any of our wave-packet inner product are as follows:

(1) Use the fact that the wave vectors are "block-diagonal" [in the sense of Eq. (11)] to reduce the τ_z to a single $(-)^j$, and to avoid any cross terms between eigenvectors from different bands.

(2) Establish an inner product of the internal band structure (e.g., $\langle \psi_k^j|\sigma_z|\psi_q^j\rangle$). Extract the translation operators to find a factor of $\exp[i(\mathbf{q}-\mathbf{k})\mathbf{x}]$ and use the inner product, a real-space integral over the sample, to produce a $\delta^d(\mathbf{q}-\mathbf{k})$.

(3) Carry out one of the momentum-space integrals to activate the Dirac delta function and reduce the problem to a single Brillouin zone.

(4) If the inner product from step 2 was a normalization condition of the internal geometry, then it produced a $(-)^j$ that, together with the sign from τ, cancels to give positive unity. Otherwise, there is a nontrivial inner product $\langle \boldsymbol{\eta}|\hat{O}|\boldsymbol{\eta}\rangle$ that must be tracked.

(5) Integrate by parts, use product rules, and use the normalization condition as necessary to manifest a factor of $|w_q|^2$ in the integrand. Interpret $|w_q|^2 \mapsto \delta^d(\mathbf{q}-\mathbf{q}_c)$ to carry out the final integral.

Before evaluating the Lagrangian proper, we have one more useful identity to compute: the expectation value of the position operator.

2. Position operator

Let us consider the self-consistency condition for the wave-packet center. This means that we require the observable $\hat{\mathbf{x}}$ to be diagonal in the wave-packet basis, with eigenvalue $\mathbf{x}_c$ for wave packet $|W(\mathbf{x}_c, \mathbf{q}_c, \boldsymbol{\eta}, t)\rangle$. Therefore,

$$\langle W|(\tau_z \otimes \sigma_z)\hat{\mathbf{x}}|W\rangle = \mathbf{x}_c\langle W|(\tau_z \otimes \sigma_z)|W\rangle. \tag{D5}$$

The bra-ket on the right then reduces to unity by the wave-packet normalization.

Before we proceed, let us define the nonabelian Berry connection

$$\hat{a}_\mu^j = \begin{pmatrix} \langle \Psi_q^0|i\sigma_z\partial_\mu\Psi_q^0\rangle & 0 \\ 0 & -\langle \Psi_q^1|i\sigma_z\partial_\mu\Psi_q^1\rangle \end{pmatrix}, \tag{D6}$$

wherein μ is a coordinate of the phase-space dynamics. We will therefore be concerned alternatively with $\hat{a}_\mathbf{x}$, $\hat{a}_\mathbf{q}$, and $\hat{a}_t$. Calculating the left-hand side of Eq. (D5) using the matrix elements of the position operator from Ref. [96], we find [97]

$$\mathbf{x}_c = \langle W|(\tau_z \otimes \sigma_z)\hat{\mathbf{x}}|W\rangle \tag{D7}$$

$$= \langle \boldsymbol{\eta}|\hat{a}_\mathbf{q}|\boldsymbol{\eta}\rangle + \frac{\partial \gamma_c}{\partial \mathbf{q}}. \tag{D8}$$

In deriving Eq. (D8), we see our first example of a noncancellation between σ_z and τ_z. The Berry connection is not *merely* the normalization condition $\langle \Psi|\sigma_z|\Psi\rangle$, and therefore cannot produce the sign needed to cancel the $(-)^j$ factor. Instead, these signs have all been contained within $\hat{a}$.

3. Extracting the electromagnetic Lagrangian

In Sec. II B, we introduced the collection of vector potentials $\mathbf{A}^j$ which encode the spin texture. Generally

speaking, the introduction of spin texture breaks the continuous translational symmetry of the (continuum limit of the) Néel ground state. Since the $\mathbf{A}^j$ are not necessarily gauge invariant, though, one expects that the translational properties of the vector potentials need not align in general with translational properties of the physical system. The situation is similar to introducing an electromagnetic vector potential in standard quantum mechanics; there, the *canonical* momentum operator $-i\partial_x$ must be adjusted to the *mechanical* momentum operator, $-i\partial_x - ieA$, where only the latter is properly conserved.

Even without explicitly computing the spin wave Hamiltonian, we expect that the kinetic energy term we explored in the two-level system will appear to undergo a sort of Peierls substitution by $\mathbf{A}^z$. With this in mind, we will now perform a gauge transformation, removing the $\mathbf{A}^z$ from the kinetic energy terms and collecting it into a new Lagrangian term which will completely encapsulate the emergent electromagnetic interaction.

Define the matrix

$$\mathcal{G} = \exp[-i(\tau_z \otimes \mathbb{1}_2)(\mathbf{A}^z \cdot \mathbf{x})]. \tag{D9}$$

Then, inserting factors of $\mathcal{G}^\dagger\mathcal{G}$ into the Lagrangian, we have

$$\langle W|\mathcal{G}^\dagger\mathcal{G}\left(i\tau_z\sigma_z\frac{d}{dt} - \mathcal{H} - A_t^z\sigma_z\right)\mathcal{G}^\dagger\mathcal{G}|W\rangle, \tag{D10}$$

where the wave packets and Hamiltonian are, at this point, still in the original gauge choice, and the brackets represent the matrix element of the operator on the diagonal in the wave-packet basis. To save space, we have removed the explicit tensor product notation. We leave it to the reader to interpret $\tau_z \mapsto \tau_z \otimes \mathbb{1}_2$ and $\sigma_z \mapsto \mathbb{1}_2 \otimes \sigma_z$ as the context demands.

The value of the transformation by $\mathcal{G}$ is not only in an internal simplification of $\mathcal{H}$, but also in elegantly extracting the emergent electromagnetic Lagrangian early in the calculation. One readily sees after carrying out the time derivative that the Lagrangian is

$$\langle\tilde{W}|\left(-(\sigma_z\dot{\mathbf{A}}^z\cdot\hat{\mathbf{x}}) - A_t^z\sigma_z + i\tau_z\sigma_z\frac{d}{dt} - \tilde{\mathcal{H}}\right)|\tilde{W}\rangle, \tag{D11}$$

where $\tilde{\mathcal{H}} = \mathcal{G}\mathcal{H}\mathcal{G}^\dagger$. Collecting the first two terms together, this can be naturally split into three components:

$$L = L_{\mathrm{EM}} + L_{dt} + L_H. \tag{D12}$$

These components represent the emergent electromagnetic, dynamical, and free-energy sectors of the spin wave equation.

The gauge transformation has also affected the wave packet itself. Concretely, the wave packet is now

$$|\tilde{W}\rangle := \mathcal{G}|W\rangle = \int d\boldsymbol{q}\, w(\boldsymbol{q},t) \times[\tilde{\eta}_0(\boldsymbol{q},t)|\Psi_0(\boldsymbol{q},t)\rangle + \tilde{\eta}_1(\boldsymbol{q},t)|\Psi_1(\boldsymbol{q},t)\rangle], \tag{D13}$$

where $|\tilde{\boldsymbol{\eta}}\rangle = (\tilde{\eta}_0, \tilde{\eta}_1)$ locates the gauge-transformed wave packet within the degenerate subspace.

From Eq. (D11), we see the need to evaluate

$$-\dot{\boldsymbol{A}}^z\cdot\langle\tilde{W}|(\mathbb{1}_2\otimes\sigma_z)\hat{\boldsymbol{x}}|\tilde{W}\rangle - A_t^z\langle\tilde{W}|\mathbb{1}_2\otimes\sigma_z|\tilde{W}\rangle \tag{D14}$$

the first of which terms will invoke a calculation analogous to those in Appendix D 2. We have

$$\langle\tilde{W}|(\mathbb{1}_2\otimes\sigma_z)\hat{\mathbf{x}}|\tilde{W}\rangle = \langle\boldsymbol{\eta}|\tau_z\hat{a}_{\mathbf{q}}|\boldsymbol{\eta}\rangle + \langle\boldsymbol{\eta}|\sigma_z|\boldsymbol{\eta}\rangle\frac{\partial\gamma_c}{\partial\mathbf{q}}. \tag{D15}$$

Substituting in the self-consistency condition (D8) on $\mathbf{x}_c$ for the γ_c derivative, we end up with

$$L_{\mathrm{EM}} = -\dot{\mathbf{A}}^z\cdot\Gamma_{\mathbf{q}} - \chi\left(\dot{\mathbf{A}}^z\cdot\mathbf{x}_c + A_t^z\right), \tag{D16}$$

where $\chi = \langle\boldsymbol{\eta}|\tau_z|\boldsymbol{\eta}\rangle$, and $\Gamma_{\mathbf{q}}$ is the covariance $\langle\boldsymbol{\eta}|\tau_z\hat{a}_{\mathbf{q}}|\boldsymbol{\eta}\rangle - \langle\boldsymbol{\eta}|\tau_z|\boldsymbol{\eta}\rangle\langle\boldsymbol{\eta}|\hat{a}_{\mathbf{q}}|\boldsymbol{\eta}\rangle$. Note that we have simplified these terms back to $\boldsymbol{\eta}$, rather than $\tilde{\boldsymbol{\eta}}$, since $\mathcal{G}$ commutes with τ_z and $\hat{a}_\mu$.

Interpreting χ as a charge, the second half of Eq. (D16) is just the interaction Lagrangian for a charged particle in an electromagnetic field [98]. Note that, in particle physics, there is also a sense in which the electromagnetic charge is a τ_z expectation value: one can rotate the isospin of a positively charged proton, through some SU(2) "isospin" space, to the neutrally charged neutron. That we have a similar sort of continuum-valued (emergent) charge is our motivation for employing the "isospin" nomenclature in our definition of $\boldsymbol{\eta}$.

4. Time derivative term

Although we have already encountered a few time derivatives without comment in the wave-packet theory, a few words are certainly in order concerning the time variable. Its treatment is one of the most delicate and subtle parts of wave-packet theory, and it is easy to make dangerous systematic errors without a proper treatment. For the reader interested in replicating our derivation, we have given some notes on the matter in Appendix D 7.

The time derivative term L_{dt} in the Lagrangian is

$$i\int d\mathbf{q}\, d\mathbf{k}\left\langle\Psi_q^i\middle|\tilde{\eta}_{i,q}^* w_q^*(\tau_z\sigma_z)\frac{d}{dt}\left(w_k\tilde{\eta}_{j,k}\middle|\Psi_k^j\right)\right\rangle. \tag{D17}$$

Since our eigenvectors are themselves block diagonal, and since $\tau_z\otimes\sigma_z$ as well as G are both diagonal, we know there can be no terms connecting $i \neq j$.

The first term (on w_k) in a product rule of expansion of Eq. (D17) is simply $\partial_t\gamma_c$. The next term, on $\tilde{\eta}_{j,k}$, generates the isospin dynamics, and the final term gives rise to matrix-valued Berry connections. All together, these terms become

$$L_{dt} = \langle\tilde{\boldsymbol{\eta}}|\dot{\mathbf{x}}_c\cdot\hat{a}_{\mathbf{x}} + \dot{\mathbf{q}}_c\cdot\hat{a}_{\mathbf{q}} + \hat{a}_t + i\partial_t|\tilde{\boldsymbol{\eta}}\rangle - \dot{\mathbf{q}}_c\cdot\mathbf{x}_c. \tag{D18}$$

We have used the self-consistency condition to replace the Berry phase term $\partial_t\gamma_c$ with $\mathbf{x}_c - \langle\boldsymbol{\eta}|\hat{a}_{\mathbf{q}}|\boldsymbol{\eta}\rangle$.

5. Hamiltonian terms

Finally, we have the terms coming from the spin wave Hamiltonian itself. These are

$$L_H = -\langle W|\mathcal{H}|W\rangle \tag{D19}$$

$$= -\frac{1}{ns}\int d\mathbf{q}\,|w_q|^2[\tilde{\eta}_i^*\tilde{\eta}_j\langle\Psi_i|\tilde{\mathcal{H}}|\Psi_j\rangle]. \tag{D20}$$

Let us define the matrix

$$\mathscr{H} = \begin{pmatrix}\langle\Psi_c^0|\tilde{\mathcal{H}}|\Psi_c^0\rangle & \langle\Psi_c^0|\tilde{\mathcal{H}}|\Psi_c^1\rangle\\ \langle\Psi_c^1|\tilde{\mathcal{H}}|\Psi_c^0\rangle & \langle\Psi_c^1|\tilde{\mathcal{H}}|\Psi_c^1\rangle\end{pmatrix}. \tag{D21}$$

One may think of $\mathscr{H}$ as a projection of the original $\mathcal{H}$ into the two-dimensional orthochronous degenerate subspace that we are now calling "isospin space," the copy of SU(2) in which $\boldsymbol{\eta}$ resides. Defining the embedding

$$E^\dagger = |\Psi_0\rangle\langle 0| + |\Psi_1\rangle\langle 1| \tag{D22}$$

which sends vectors in the isospin subspace to their representation in parent 4×4 Hilbert space space, $\mathscr{H}$ is merely

$$\tilde{\mathscr{H}} = E\tilde{\mathcal{H}}E^\dagger. \tag{D23}$$

This Hermitian matrix will govern the dynamics of $|\tilde{\boldsymbol{\eta}}\rangle$ in the semiclassical dynamics we are about to describe. The total contribution from these energy terms to the wave-packet Lagrangian is, simply,

$$L_H = -\langle\tilde{\boldsymbol{\eta}}|\tilde{\mathscr{H}}|\tilde{\boldsymbol{\eta}}\rangle. \tag{D24}$$

6. Phase-space EOM

Let us take stock of our progress. We have a Lagrangian of three terms, which have been reduced to

$$L_{\rm EM} = -\dot{\mathbf{A}}^z\cdot\Gamma_{\mathbf{q}} - \chi\left(\dot{\mathbf{A}}^z\cdot\mathbf{x}_c + A_t^z\right), \tag{D25a}$$

$$L_{dt} = \langle\tilde{\boldsymbol{\eta}}|\dot{\mathbf{x}}_c\cdot\hat{a}_{\mathbf{x}} + \dot{\mathbf{q}}_c\cdot\hat{a}_{\mathbf{q}} + \hat{a}_t + i\partial_t|\tilde{\boldsymbol{\eta}}\rangle - \dot{\mathbf{q}}_c\cdot\mathbf{x}_c, \tag{D25b}$$

$$L_H = -\langle\tilde{\boldsymbol{\eta}}|\tilde{\mathscr{H}}|\tilde{\boldsymbol{\eta}}\rangle. \tag{D25c}$$

Now, we can take variations against $\mathbf{x}_c$, $\mathbf{q}_c$, and $|\boldsymbol{\eta}\rangle$ to derive semiclassical equations of motion (EOM).

First, let us find the force equation by taking a variation against $\mathbf{x}_c$. For the Lorentz force term, we unsurprisingly have

$$\frac{\delta L_A}{\delta x_c^\mu} = -\chi\left[\partial_t A_\mu^z + \partial_{x_c^\mu}A_t^z + \dot{\mathbf{x}}_c\cdot\partial_{x_c^\mu}\mathbf{A}^z - (\dot{\mathbf{x}}_c\cdot\boldsymbol{\nabla})A_\mu^z\right] \tag{D26}$$

$$= \chi\mathbf{E} + \chi\dot{\mathbf{x}}_c\times\mathbf{B}, \tag{D27}$$

where we define the fields $\mathbf{E} = -\boldsymbol{\nabla}A_t^z - \partial_t\mathbf{A}^z$ and $\mathbf{B} = \boldsymbol{\nabla}\times\mathbf{A}^z$ in the obvious ways. The time derivative term meanwhile gives

$$\frac{\delta L_{dt}}{\delta x_c^\mu} = -\dot{\mathbf{q}}_c + \left\langle\Omega_{\mu\nu}^{xx}\right\rangle\dot{x}_c^\nu + \left\langle\Omega_{\mu\nu}^{xq}\right\rangle\dot{q}_c^\nu + \left\langle\Omega_\mu^{xt}\right\rangle, \tag{D28}$$

where

$$\left\langle\Omega_{\mu\nu}^{\alpha\beta}\right\rangle = \langle\boldsymbol{\eta}|\left(\frac{\partial\hat{a}_{\beta^\nu}}{\partial\alpha^\mu} - \frac{\partial\hat{a}_{\alpha^\mu}}{\partial\beta^\nu}\right)|\boldsymbol{\eta}\rangle \tag{D29}$$

is the $\boldsymbol{\eta}$-density trace of the nonabelian Berry curvature, as discussed in Ref. [53].

Finally, we have a contribution from the gauged Hamiltonian. In most cases we consider in this paper, no such terms survive at $O(|\mathbb{A}|^2)$; the terms that might nominally survive are those wrapped encoded in $L_{\rm EM}$. Examples of terms that may survive and not be included in $L_{\rm EM}$ could include spatially dependent anisotropy or DMI, arising from, e.g., wedge-shaped layers in magnetic heterostructures. Taking this term and the Lorentz force together, the force equation is

$$\dot{\mathbf{q}}_c = \mathrm{Tr}\left[\hat{\rho}\left(\tau_z(\mathbf{E} + \dot{\mathbf{x}}_c\times\mathbf{B}) - \frac{\partial\mathcal{E}}{\partial\mathbf{x}_c}\right)\right], \tag{D30}$$

where $\mathcal{E}$ is the energy of the unperturbed degenerate bands, and where we have defined the density operator

$$\hat{\rho} = \rho_0|0\rangle\langle 0| + \rho_1|1\rangle\langle 1|. \tag{D31}$$

Now, we turn to the velocity equation. The results are little different from what we would expect from standard nonabelian wave-packet theory, giving us the classical velocity together with Berry-curvature-induced transverse velocities

$$\dot{\mathbf{x}}_c = \mathrm{Tr}[\hat{\rho}(\partial_{\mathbf{q}}\mathcal{E} + \boldsymbol{\Omega}^{qq}\dot{\mathbf{q}}_c + \boldsymbol{\Omega}^{qx}\dot{\mathbf{x}}_c + \boldsymbol{\Omega}^{qt})]. \tag{D32}$$

Now, we turn to the most interesting equation of motion, generated by the variation again $\langle\boldsymbol{\eta}|$. This generates terms of the form

$$\frac{\delta L_{\rm EM}}{\delta\tilde{\boldsymbol{\eta}}^*} = -\dot{\mathbf{A}}^z\cdot\frac{\delta\Gamma_{\mathbf{q}}}{\delta\tilde{\boldsymbol{\eta}}^*} - (\dot{\mathbf{A}}^z\cdot\mathbf{x}_c)\tau_z\tilde{\boldsymbol{\eta}} - A_t^z\tau_z\tilde{\boldsymbol{\eta}}, \tag{D33}$$

$$\frac{\delta\Gamma_{\mathbf{q}}}{\delta\tilde{\boldsymbol{\eta}}^*} = \tau_z\hat{a}_{\mathbf{q}}\tilde{\boldsymbol{\eta}} - \tau_z(\langle\tilde{\boldsymbol{\eta}}|\hat{a}_{\mathbf{q}}|\tilde{\boldsymbol{\eta}}\rangle)\tilde{\boldsymbol{\eta}} - \chi\hat{a}_{\mathbf{q}}\tilde{\boldsymbol{\eta}}, \tag{D34}$$

$$\frac{\delta L_{dt}}{\delta\tilde{\boldsymbol{\eta}}^*} = \left[\dot{\mathbf{q}}_c\cdot\hat{a}_{\mathbf{q}} + i\frac{\partial}{\partial t}\right]\tilde{\boldsymbol{\eta}}, \tag{D35}$$

$$\frac{\delta L_H}{\delta\tilde{\boldsymbol{\eta}}^*} = -\mathscr{H}\tilde{\boldsymbol{\eta}}. \tag{D36}$$

The final general equation of motion is

$$i\left(\frac{d}{dt} + \mathscr{A}_t\right)\boldsymbol{\eta} = \left[\mathscr{H} + \tau_z A_t^z + \hat{V}_\chi\right]\boldsymbol{\eta}, \tag{D37}$$

where $\mathscr{H} = E\mathcal{H}E^\dagger$ (note that we have removed the gauge transformation $\mathcal{G}$), $\mathscr{A}$ is the time-covariant connection on phase space

$$\mathscr{A}_t = \dot{\mathbf{q}}_q\cdot\hat{a}_{\mathbf{q}} + \dot{\mathbf{x}}_c\cdot\hat{a}_{\mathbf{x}} + \hat{a}_t, \tag{D38}$$

$$\mathscr{A}_t^{ij} = \left\langle\psi_c^i\right|i\sigma_z\frac{d}{dt}\left|\psi_c^j\right\rangle, \tag{D39}$$

and $\hat{V}_\chi$ is a nonlinear term deriving from $\Gamma_{\mathbf{q}}$. It is given by

$$\hat{V}_\chi = -\dot{\mathbf{A}}^z\cdot(\tau_z\hat{a}_{\mathbf{q}} - \tau_z\hat{P}_\eta\hat{a}_{\mathbf{q}} - \hat{a}_{\mathbf{q}}\hat{P}_\eta\tau_z), \tag{D40}$$

where $\hat{P}_\eta = |\boldsymbol{\eta}\rangle\langle\boldsymbol{\eta}|$ is the projector onto the isospin state, and as before the dot product (with $\dot{\mathbf{A}}^z$) is taken with the subscript in $\hat{a}_{\mathbf{q}}$. This potential is nonlinear in the sense that, through $\hat{P}_\eta$, it depends quadratically on the current state, and the resulting term in the Hamiltonian has the schematic form $|\psi|^2|\psi\rangle$. However, this nonlinear term balances precipitously on the edge of irrelevance. $\dot{\mathbf{A}}^z$ is itself $O(\mathbb{A}^2)$, so this term survives only if $\hat{a}_{\mathbf{q}}$ is $O(\mathbb{A}^0)$. Although there is no reason (to our knowledge) this could not happen in principle, none of the concrete systems we consider later in the paper can activate this term. What is more, the term would seem only relevant in the case of a moving spin texture, so that $\dot{\mathbf{A}}^z$ is nonzero. Such a term may be of interest for those working in the dynamics of AFM solitons, but we leave that to future research.

7. Notes on time derivatives in wave-packet theory

There are two variables, $\mathbf{x}$ and $\mathbf{q}$, that have been floating around as dummy variables of integration in some of our calculations. Several functions, such as the wave-packet envelope $a_q = a(\mathbf{q}, t)$ or the Bloch eigenvectors $e^{i\mathbf{q}\mathbf{x}}u(\mathbf{q}, t)$, are functions of both $\mathbf{q}$ (or $\mathbf{x}$) and time. For these functions, there is no difference between a total time derivative and a partial time derivative because $\mathbf{q}$ and $\mathbf{x}$ are clearly independent

variables (merely coordinates of a space) that do not, themselves, possess any temporal dynamics.

On the other hand, the gauge field $\mathbf{A}^z = \mathbf{A}^z(\mathbf{x}_c, t)$ was originally, and will always be, evaluated at $\mathbf{x}_c$ in its spatial argument. This $\mathbf{x}_c$ is a dynamical variable, which does depend on time and has dynamics. Our notation, which follows Ref. [55], is that a partial time derivative of such a function acts only on the second argument slot, where there is an explicit time dependence. A total time derivative, on the other hand, would include the time dependence through $\mathbf{x}_c$, so that

$$\frac{d}{dt} = \frac{\partial}{\partial t} + \dot{\boldsymbol{x}}_c \cdot \frac{\partial}{\partial \boldsymbol{x}_c}. \tag{D41}$$

So far, our discussion has perhaps clarified the notation, but is by no means unusual. The delicacy of these operations in wave-packet theory occurs when evaluation of a wave-packet expectation value promotes a function in the integrand, where it may have possessed only an explicit time dependence, to a function of $\mathbf{q}_c(t)$, due to the firing of the Dirac delta function $|a_q|^2$. The question is as follows: Should the time derivative under the integrand be lifted to a total time derivative or a partial time derivative once the function acquires a new time dependence in the phase-space coordinate arguments $\mathbf{x}_c(t)$ and $\mathbf{q}_c(t)$?

The answer is that we must promote it to a partial time derivative. The original, physical meaning of such a time derivative in the integrand was to ask how, at any given point in space, a function changed with time. We are concerned with *the function's temporal behavior*, not the temporal behavior of the combined wave-packet/function system. From a different perspective, we note that we are certainly free to take the time derivative as early as possible. Suppose we "carry out" the time derivative in the integrand by replacing $\partial_t f(t, \mathbf{q})$ with its formal derivative $F(t, \mathbf{q})$. Now, F is just a function which we have determined in principle before ever introducing the phase-space path $(\mathbf{x}_c, \mathbf{q}_c)$, so after firing the Delta function we simply have $F(t, \mathbf{q}_c(t))$. Clearly, $F(t, \mathbf{q}_c(t)) = \partial_t f(t, \mathbf{q}_c(t))$, with the derivative only in the first argument.

APPENDIX E: STAGGERED ORDER

Suppose we changed the basis of Eq. (6) by a Hadamard matrix

$$M = \frac{1}{2}\begin{pmatrix} 1 & 1 \\ 1 & -1 \end{pmatrix}, \tag{E1}$$

sending α and β to $\delta m = m_x + i m_y$ and $\delta n = n_x + i n_y$, respectively. Neglecting anisotropy for the moment, the resulting Schrödinger equation on $\hat{h}$ is

$$i\sigma_x \frac{d}{dt}\begin{bmatrix} \delta m \\ \delta n \end{bmatrix} = \frac{1}{2}\left[Z + \sigma_z(Z - J\nabla^2)\right]\begin{bmatrix} \delta m \\ \delta n \end{bmatrix}. \tag{E2}$$

Neglecting the dynamics of δm, this can be solved by taking a second time derivative and plugging the original equation for $\dot{n}$ into the new equation for $\ddot{n}$. The result is

$$0 = \left(\frac{1}{c^2}\frac{d^2}{dt^2} - \nabla^2\right)\delta n, \tag{E3}$$

where $c = \sqrt{ZJ/2}$. Therefore, our σ_z-measured Schrödinger dynamics given (in either of the equivalent 2×2 blocks) by Eq. (5) are in fact equivalent (in this simple regime, at least) to the Klein-Gordon–type second-order dynamics found more commonly in the literature. It is no surprise that relativistic dynamics describes the system whose modes, as we have seen, are restricted to timelike points in a hyperboloid of two sheets. In the case where $K = 0$, we actually have massless particles, the hyperboloid of two sheets becomes a light cone. Adding the anisotropy restores a mass term $(\Box - m^2)\delta n = 0$ to the Klein-Gordon equation, just as it opens a mass gap in our hyperboloid.

[1] R. Cheng, J. Xiao, Q. Niu, and A. Brataas, Phys. Rev. Lett. **113**, 057601 (2014).

[2] M. W. Daniels, W. Guo, G. M. Stocks, D. Xiao, and J. Xiao, New J. Phys. **17**, 103039 (2015).

[3] N. Kanda, T. Higuchi, H. Shimizu, K. Konishi, K. Yoshioka, and M. Kuwata-Gonokami, Nat. Commun. **2**, 362 (2011).

[4] A. V. Kimel, A. Kirilyuk, P. A. Usachev, R. V. Pisarev, A. M. Balbashov, and T. Rasing, Nature (London) **435**, 655 (2005).

[5] T. Satoh, S.-J. Cho, R. Iida, T. Shimura, K. Kuroda, H. Ueda, Y. Ueda, B. A. Ivanov, F. Nori, and M. Fiebig, Phys. Rev. Lett. **105**, 077402 (2010).

[6] S. Seki, T. Ideue, M. Kubota, Y. Kozuka, R. Takagi, M. Nakamura, Y. Kaneko, M. Kawasaki, and Y. Tokura, Phys. Rev. Lett. **115**, 266601 (2015).

[7] Y. Shiomi, R. Takashima, D. Okuyama, G. Gitgeatpong, P. Piyawongwatthana, K. Matan, T. J. Sato, and E. Saitoh, Phys. Rev. B **96**, 180414 (2017).

[8] Y. Shiomi, R. Takashima, and E. Saitoh, Phys. Rev. B **96**, 134425 (2017).

[9] G. Gitgeatpong, Y. Zhao, P. Piyawongwatthana, Y. Qiu, L. W. Hariger, N. P. Butch, T. J. Sato, and K. Matan, Phys. Rev. Lett. **119**, 047201 (2017).

[10] R. Cheng, X. Wu, and D. Xiao, Phys. Rev. B **96**, 054409 (2017).

[11] R. Cheng, M. W. Daniels, J.-G. Zhu, and D. Xiao, Sci. Rep. **6**, 24223 (2016).

[12] J. Lan, W. Yu, and J. Xiao, Nat. Commun. **8**, 178 (2017).

[13] E. G. Tveten, A. Qaiumzadeh, and A. Brataas, Phys. Rev. Lett. **112**, 147204 (2014).

[14] S. K. Kim, Y. Tserkovnyak, and O. Tchernyshyov, Phys. Rev. B **90**, 104406 (2014).

[15] O. Gomonay, V. Baltz, A. Brataas, and Y. Tserkovnyak, Nat. Phys. **14**, 213 (2018).

[16] S. K. Kim, O. Tchernyshyov, and Y. Tserkovnyak, Phys. Rev. B **92**, 020402 (2015).

[17] A. Qaiumzadeh, L. A. Kristiansen, and A. Brataas, Phys. Rev. B **97**, 020402 (2018).

[18] R. Cheng, S. Okamoto, and D. Xiao, Phys. Rev. Lett. **117**, 217202 (2016).

[19] V. A. Zyuzin and A. A. Kovalev, Phys. Rev. Lett. **117**, 217203 (2016).

[20] F. Keffer and C. Kittel, Phys. Rev. **85**, 329 (1952).

[21] T. Liu and G. Vignale, Phys. Rev. Lett. **106**, 247203 (2011).

[22] A. Khitun, M. Bao, and K. L. Wang, J. Phys. D: Appl. Phys. **43**, 264005 (2010).

[23] Others have proposed using the phase to encode information directly [22], though these schemes sometimes end up using spin wave amplifiers anyway. In any case, a natural design pattern would seem to use either the phase for computing and the amplitude for memory, or vice versa, and so the amplitude will somewhere need to be restored from some suppressed state.

[24] A. A. Sawchuk and T. C. Strand, Proc. IEEE **72**, 758 (1984).

[25] As the magnonic isospin lives in a noncommutative space, device components in an isospin computing architecture will not commute in general. *nonabelian* is a synonym for *non-commutative*: hence, the name.

[26] T. Schneider, A. A. Serga, B. Leven, B. Hillebrands, R. L. Stamps, and M. P. Kostylev, Appl. Phys. Lett. **92**, 022505 (2008).

[27] A. V. Chumak, V. I. Vasyuchka, A. A. Serga, and B. Hillebrands, Nat. Phys. **11**, 453 (2015).

[28] E. G. Tveten, T. Müller, J. Linder, and A. Brataas, Phys. Rev. B **93**, 104408 (2016).

[29] The literature is typically consistent with maintaining factors of either $\frac{1}{2}$ or 1 in front of the various terms of Eq. (3), but avoids mixing them; see for instance Refs. [28] or [99]. Since we have expressed the free energy in terms of the sublattices, rather than the staggered order $\mathbf{n}$ and the local magnetization $\mathbf{m}$, we will instead opt to disperse our factors of $\frac{1}{2}$ symmetrically in Eq. (1b) and require the reader to perform the conversion between conventions if needed.

[30] $\mathbf{n}$ is the order parameter for antiferromagnets, and so AFM dynamics are often (though not in the present paper) described using $\mathbf{n}$ as the primary dynamical variable. Our description of spin wave fields in terms of the sublattices, rather than $\mathbf{n}$, will preserve the first-order (in time) nature of the Landau-Lifshitz equation instead of passing over to the second-order Klein-Gordon equation governing staggered order fluctuations. Maintaining a first-order theory facilitates the use of wave-packet theory that we introduce in Appendix D.

[31] Note that this separation into slow and fast variables is exact within linear spin wave theory; likewise when we substitute the slow modes $\pm\hat{z}$ for $\pm R\hat{z}$ come the introduction of spin texture.

[32] This comes with the understanding that the real part must be taken to recover the physical fields; for example, $m_A^x = \mathrm{Re}[\alpha_+ + \alpha_-]/\sqrt{2}$.

[33] Formally, this basis is $\{\partial_{m_A^x} - i\partial_{m_A^y}, \partial_{m_B^x} - i\partial_{m_B^y}, \partial_{m_A^x} + i\partial_{m_A^y}, \partial_{m_B^x} + i\partial_{m_B^y}\}$, where ∂_μ is the basis vector induced by the coordinate μ in tangent space. Note that, though we define $\alpha_\pm$ as conjugates in the main text, it is actually the underlying basis vectors that are conjugate. This is the sense in which $\alpha_\pm$ and $\beta_\pm$ can be treated as independent variables.

[34] V. K. Dugaev, P. Bruno, B. Canals, and C. Lacroix, Phys. Rev. B **72**, 024456 (2005).

[35] K. Y. Guslienko, G. R. Aranda, and J. M. Gonzalez, Phys. Rev. B **81**, 014414 (2010).

[36] A. Mostafazadeh, Classical Quantum Gravity **20**, 155 (2003).

[37] J. Colpa, Phys. A (Amsterdam) **93**, 327 (1978).

[38] R. Shindou, R. Matsumoto, S. Murakami, and J.-i. Ohe, Phys. Rev. B **87**, 174427 (2013).

[39] I. Proskurin, R. L. Stamps, A. S. Ovchinnikov, and J.-i. Kishine, Phys. Rev. Lett. **119**, 177202 (2017).

[40] R. P. Cameron and S. M. Barnett, New J. Phys. **14**, 123019 (2012).

[41] Given that the isospin distinguishes between underlying fields which are complex conjugates of each other, one may wonder whether flipping the isospin is associated with charge conjugation. Indeed, we will see later in Eqs. (27) that the expectation value of τ_z gives us the effective charge in response to an effective electromagnetic field. This sort of dynamical electric charge is what inspired our borrowing of the term "isospin" from particle physics.

[42] K. Nakata, J. Klinovaja, and D. Loss, Phys. Rev. B **95**, 125429 (2017).

[43] K. A. van Hoogdalem, Y. Tserkovnyak, and D. Loss, Phys. Rev. B **87**, 024402 (2013).

[44] R. Cheng and Q. Niu, Phys. Rev. B **86**, 245118 (2012).

[45] K. Nakata, S. K. Kim, J. Klinovaja, and D. Loss, Phys. Rev. B **96**, 224414 (2017).

[46] P. M. Buhl, F. Freimuth, S. Blügel, and Y. Mokrousov, Phys. Status Solidi (RRL) **11**, 1700007 (2017).

[47] We take these to be the real-valued generators, so that the rotation by θ about $\hat{e}_j$ given through the exponential map $\exp(\theta J_j)$. Some authors include an i in this expression for the rotation matrix in order to make it look manifestly "unitary," and those authors must also have imaginary-valued J_j matrices to compensate.

[48] S. Rohart and A. Thiaville, Phys. Rev. B **88**, 184422 (2013).

[49] Depending on Moriya's rules [100] for how a system breaks inversion symmetry, the vector structure of the free-energy term may differ, but will in general descend from some lattice Hamiltonian $\sum_{\langle ij\rangle} \mathbf{D}_{ij} \cdot (\mathbf{m}_A{}^i \times \mathbf{m}_B{}^j)$.

[50] This length scale is set when D is large enough to influence the spin texture; the critical value of D is typically set by anisotropy. So, if D is large enough to influence the texture, then it is order $|\mathbb{A}|$, and otherwise we are harmlessly overestimating the importance of contributions from D.

[51] Note that $R\mathbf{m}$ has no $\hat{z}$ component since $\mathbf{m} \perp \mathbf{n}$ by construction.

[52] See Supplemental Material at http://link.aps.org/supplemental/10.1103/PhysRevB.98.134450 for *Mathematica* tools for computing generic spin wave Hamiltonians.

[53] D. Culcer, Y. Yao, and Q. Niu, Phys. Rev. B **72**, 085110 (2005).

[54] M.-C. Chang and Q. Niu, Phys. Rev. Lett. **75**, 1348 (1995).

[55] G. Sundaram and Q. Niu, Phys. Rev. B **59**, 14915 (1999).

[56] C. Zhang, A. M. Dudarev, and Q. Niu, Phys. Rev. Lett. **97**, 040401 (2006).

[57] D. Xiao, M.-C. Chang, and Q. Niu, Rev. Mod. Phys. **82**, 1959 (2010).

[58] R. Matsumoto and S. Murakami, Phys. Rev. Lett. **106**, 197202 (2011).

[59] R. Shindou and K.-I. Imura, Nucl. Phys. B **720**, 399 (2005).

[60] Reference [59] deals with a nonabelian gauge field in the nonabelian wave-packet theory, but only to derive it implicitly from the band structure; that is, they do not write such a gauge field in their starting Lagrangian, but instead tease it out. Our approach is more similar to the original technique by Ref. [101], but lifted to the nonabelian case (and of course to the non-Euclidean Hilbert space). These two approaches

should ultimately agree, though each is operationally preferable for certain classes of problems.
[61] As long as the wave packet satisfies the assumptions listed in the main text, the functional form of the wave packet does not affect the outcome of wave-packet theory.
[62] N. Nagaosa and Y. Tokura, Nat. Nanotechnol. **8**, 899 (2013).
[63] Y. Gao, S. A. Yang, and Q. Niu, Phys. Rev. Lett. **112**, 166601 (2014).
[64] Y. Gao, S. A. Yang, and Q. Niu, Phys. Rev. B **91**, 214405 (2015).
[65] M. Tinkham, *Group Theory and Quantum Mechanics* (Dover, New York, 2010).
[66] As usual, there are two distinct SU(2) rotations corresponding to the O(3) rotation R^{-1} of the ground state. They differ by a sign, but this sign is immaterial in calculations of observable quantities such as m_z.
[67] The constant ($\mathbb{1}_2$) part is familiarly unimportant in a truly 1D system, but with multibranch devices such as the one in Fig. 6 it introduces a *very much important* relative U(1) phase between different spin wave channels.
[68] E. Gomonai, B. Ivanov, V. L'vov, and G. Oksyuk, Zh. Eksp. Teor. Fiz. **97**, 307 (1990) [Sov. Phys. JETP **70**, 307 (1990)].
[69] N. Papanicolaou, Phys. Rev. B **51**, 15062 (1995).
[70] B. A. Ivanov and A. K. Kolezhuk, Phys. Rev. Lett. **74**, 1859 (1995).
[71] N. Manton and P. Sutcliffe, *Topological Solitons*, Cambridge Monographs on Mathematical Physics (Cambridge University Press, Cambridge, 2004)
[72] There is no temporal index because the DW is assumed to be static.
[73] We use the parameters from Ref. [12]. Converting their parameters to our notation gives $J_{\mathrm{AF}} = 7.25\ \mathrm{nm}^2\,\mathrm{ps}^{-1}$, $2J_{\mathrm{F}} = 0.0221\ \mathrm{ps}^{-1}$, $\lambda = 29.1$ nm, $|\mathbf{D}| = 0.663\ \mathrm{nm\,ps}^{-1}$.
[74] Naturally, it cannot express magnon-magnon interactions in that state.
[75] Since margins of error in these works are not given, we simply take their results as exact. Reference [12], for instance, says that a 16.2-GHz drive frequency produces a quarter wave plate, whereas our calculations require a 17.1-GHz drive, an error of $\sim$5%.
[76] In fact, this is not much of a surprise since the SAF domain wall essentially acts as a local hard axis anisotropy, and we saw in Fig. 5 that the SAF domain wall acted as a σ_x rotator as well.
[77] R. Khymyn, I. Lisenkov, V. S. Tiberkevich, A. N. Slavin, and B. A. Ivanov, Phys. Rev. B **93**, 224421 (2016).
[78] S. Banerjee, J. Rowland, O. Erten, and M. Randeria, Phys. Rev. X **4**, 031045 (2014).
[79] R. Cheng, D. Xiao, and A. Brataas, Phys. Rev. Lett. **116**, 207603 (2016).
[80] J. Chęciński, M. Frankowski, and T. Stobiecki, Phys. Rev. B **96**, 174438 (2017).
[81] A. Slavin and V. Tiberkevich, IEEE Trans. Magn. **45**, 1875 (2009).
[82] R. Khymyn, I. Lisenkov, V. Tiberkevich, B. A. Ivanov, and A. Slavin, Sci. Rep. **7**, 43705 (2017).
[83] J. A. Acebrón, L. L. Bonilla, C. J. Pérez Vicente, F. Ritort, and R. Spigler, Rev. Mod. Phys. **77**, 137 (2005).
[84] F. A. Rodrigues, T. K. D. Peron, P. Ji, and J. Kurths, Phys. Rep. **610**, 1 (2016).
[85] A. Altland and B. Simons, *Condensed Matter Field Theory*, 2nd ed. (Cambridge University Press, Cambridge, 2010).
[86] T. Frankel, *The Geometry of Physics: An Introduction* (Cambridge University Press, Cambridge, 2011).
[87] O. Tchernyshyov, Ann. Phys. **363**, 98 (2015).
[88] For instance, one could add collective coordinate sectors to the Lagrangian we present here, and the new Lagrangian would then, in principle, encode magnon-soliton dynamics. We leave that procedure to future research.
[89] Such terms would need to be reserved for coupling to a Lagrangian collective coordinate theory of the textural dynamics, which we do not treat here.
[90] To be precise, $\mathbb{A}$ is strictly determined up to its topological charge, i.e., up to the sectors defined in Ref. [102].
[91] Though, not the unique mechanism: see hard-axis anisotropy.
[92] We are dealing only with the $\hat{z}$ component since we will generally not work in higher than $(2+1)$ dimensions and therefore the magnetic field has only one component, hence the dot product by $\hat{z}$.
[93] R. Cheng, arXiv:1012.1337.
[94] Y.-Q. Ma, S. Chen, H. Fan, and W.-M. Liu, Phys. Rev. B **81**, 245129 (2010).
[95] F. Piéchon, A. Raoux, J.-N. Fuchs, and G. Montambaux, Phys. Rev. B **94**, 134423 (2016).
[96] E. Blount, Solid State Phys. **13**, 305 (1962).
[97] A guide to carrying out this type of calculation, albeit without the hyperbolic factors, can be found in the Appendix of Ref. [55].
[98] J. D. Jackson, *Classical Electrodynamics*, 3rd ed. (Wiley, New York, 2007).
[99] K. M. D. Hals, Y. Tserkovnyak, and A. Brataas, Phys. Rev. Lett. **106**, 107206 (2011).
[100] T. Moriya, Phys. Rev. **120**, 91 (1960).
[101] M.-C. Chang and Q. Niu, Phys. Rev. B **53**, 7010 (1996).
[102] A. A. Belavin and A. M. Polyakov, Pis'ma Zh. Eksp. Teor. Fiz. **22**, 503 (1975) [JETP Lett. **22**, 245 (1975)].